The copyright of this thesis vests in the author. No quotation from it or information derived from it is to be published without full acknowledgement of the source. The thesis is to be used for private study or non-commercial research purposes only.

Published by the University of Cape Town (UCT) in terms of the non-exclusive license granted to UCT by the author.

University of Cape Town

GROUNDWATER REDOX CONDITIONS AT A PETROLEUM CONTAMINATED SITE, KUILS RIVER, SOUTH AFRICA: PATHWAYS FOR BTEX BIODEGRADATION

A Dissertation Presented to
The Academic Faculty

by

Greg Lee Merrett
BSc. (Hons) Geology, University of Natal

Submitted in Partial Fulfilment of the requirements for the degree of
Master of Science in Environmental Geochemistry

Department of Geological Sciences
University of Cape Town
December 2003

University of Cape Town

ABSTRACT

A shallow sandy aquifer, contaminated by petrol from an underground storage tank, was studied to determine if intrinsic bioremediation of the hydrocarbons is taking place. Groundwater samples taken from 32 monitoring wells were analysed for NO_3^-, NH_4^+, Mn^{2+}, Fe^{2+}, SO_4^{2-}, and ΣH_2S. Portable electrodes were used to make field measurements of electrical conductivity, redox potential, and pH. The variation and distribution of these redox-sensitive groundwater constituents show that bioremediation via NO_3^- reduction, Fe^{3+} reduction, and SO_4^{2-} reduction (and possibly methanogenesis in the most reduced part of the plume) is occurring. In some cases redox processes are taking place simultaneously resulting in redox zones that overlap. Iron and sulphate reduction are the dominant processes taking place.

Sediments incubations carried out over 48 hours in two samples were carried out order to determine the rates of iron and sulphide reduction. The highest iron reduction rate (FeRR) measured as the accumulation of extractable Fe^{2+} was 99 $nmol.cm^{-3}.h^{-1}$ and provides evidence for the occurrence of concomitant Fe^{3+} and SO_4^{2-} reduction. The maximum sulphate reduction rate (SRR) measured was 178 $nmol.cm^{-3}.h^{-1}$. It is proposed that the SO_4^{2-} concentration rather than the reactivity of organic matter is responsible for determining the SRR.

Generally an increase in the pH and alkalinity within the contaminant plume has been found in similar studies carried out previously. This has not been observed at the sire currently under investigation and has yet to be explained. Background water samples are oversaturated with respect to calcite and undersaturated with respect to iron sulphide phases. The opposite is generally observed in samples taken from within the plume.

University of Cape Town

The availability of terminal electron acceptors (TEA's) is considered to be the limiting factor for bioremediation. Future biological remedial activities involving the injection of NO_3^- or SO_4^{2-} should therefore be considered.

University of Cape Town

ACKNOWLEDGEMENTS

I would like to express my gratitude and sincere thanks to the following people without whom the successful completion of this project would not have been possible:

- My Supervisor, Dr A.N. Roychoudhury, for his guidance and invaluable insight into the project.

- Mr Ross Campbell from Kantey and Templer Consulting Engineers, who's idea it was to undertake the project in the first place. Thank you for your time and effort that was involved in organising the project, for always taking the time out to discuss various aspects, and for proof reading parts of the project.

- Engen for providing funding for the project.

- To Meris Smith for her input, ideas, discussion regarding the project, and for always been willing to help regardless of what the crisis is.

- Mr Patrick Sieas for his assistance in running the IC sample analyses, and for maintaining an adequate supply of deionised water in the laboratory throughout the duration of the project.

- Margaret and Michael McNair, for providing me with accommodation during my period of study in Cape Town.

University of Cape Town

- My family and friends for providing me with the necessary support and encouragement that was required in order to make the decision to resign and pursue my studies further. Thank you for believing in me and for all your support over the years, to you I am forever indebted.

- To my classmates for what can only be described as a testing year. I would like to thank Ruth Mitchell and Michael Starke for helping in the field. A special word of thanks to Jacques Peterson who sacrificed many days of his own valuable time to assist me in the field with sample collection.

- The Corner House for providing welcome refreshment on Friday nights. Without the sweet sounds that filled my ears maintaining sanity during this project would have been very difficult.

University of Cape Town

TABLE OF CONTENTS

University of Cape Town

University of Cape Town

University of Cape Town

LIST OF TABLES

University of Cape Town

LIST OF FIGURES

University of Cape Town

University of Cape Town

ABBREVIATIONS

AAS: Atomic absorption spectrometry

AVS: Acid volatile sulphides (FeS)

BTEX: Benzene, toluene, ethylbenzene, o-, m-, and p-xylene.

DOC: Dissolved organic carbon

EC: Electrical conductivity

E_h: Redox potential

EN: Electroneutrality

FeRR: Iron reduction rate

FPP: Free phase product – refers to petroleum that occurs on top of the water table as a result of the density differences between the two phases.

IC: Ion Chromatography

Pe: Electron activity

SRR: Sulphate reduction rate

TEA: Terminal electron acceptor

TEAP: Terminal electron accepting processes

ΣH_2S: Total dissolved S(-II)

University of Cape Town

CHAPTER 1 - INTRODUCTION AND REVIEW OF PROCESSES OCCURRING IN HYDROCARBON CONTAMINATED AQUIFERS

1. INTRODUCTION

The leakage of petroleum hydrocarbons into the groundwater is a common problem and influences groundwater quality. This presents a risk, and a great deal of concern is associated with the impact of hydrocarbons on humans and the recipient environment (Krumholz *el. al.*, 1996). The biodegradation of aromatic hydrocarbons (BTEX) in petroleum is especially of concern as they are the most water-soluble fraction of petroleum (Fetter, 1999, Krumholz, 1996). The risk of exposure is further amplified by the fact that benzene is a known carcinogen (Chapelle, 1993).

The concept of natural or intrinsic bioremediation is defined by Borden (1994) as follows: "...to allow naturally occurring microorganisms to degrade contaminants that have been released into the subsurface and at the same time to minimise risks to public health and the environment. Use of this approach will require an assessment of those factors that influence the biodegradation capacity of an aquifer ...". The susceptibility of hydrocarbons to metabolism by aerobic and anaerobic microorganisms is a major factor controlling their transport and fate (Krumholz, 1996), while understanding the fate and distribution of redox processes is also fundamental to predicting the fate and transport of chemical contaminants in groundwater systems (Chapelle *et al.*, 1996). In order to evaluate the risk, to design groundwater monitoring programmes, and to perform remedial action, a detailed understanding of the attenuation processes in a contaminant plume is required (Bjerg *et al.*, 1995).

University of Cape Town

In order to assess intrinsic bioremediation, one of the most important questions that needs to be addressed is whether the compounds of concern are biodegrading and there are various ways to address this issue. The simplest way is to determine from the groundwater monitoring data, if there is a decline in the total mass of the contaminant as the plume migrates downgradient (Borden, 1994). There are however problems associated with this as it requires an extensive monitoring well network. Furthermore, dispersion may result in reduced point concentrations. Therefore, comparison of dissolved hydrocarbon concentrations at individual points is not sufficient to prove biodegradation (Borden, 1994).

Another method that has been extensively used in studies of this nature is to monitor the changes in concentration of inorganic compounds. Variations in the concentrations of elements with variable oxidation states and the development of the redox concept in contaminant plumes was introduced in the late 1970's by Baedecker and Back (1979), and Champ *et al.* (1979). Petroleum hydrocarbons are known to be highly biodegradable (Aelion, 1996) and the development of redox zones associated with the contaminant plume is well documented (Bjerg *et al.*, 1995; Cozzarelli *et al.*, 2001; Lyngkilde & Christensen, 1992; Norkus *et al.*, 1996).

University of Cape Town

The development of these redox zones occurs as a result of bacteria oxidising BTEX and other organic pollutants. In the process, electrons are transferred from the susceptible contaminants to inorganic electron acceptors. Usable energy is recovered during this electron transfer process (Krumholz *et al.*, 1996). An observable redox zonation may result as redox reactions in natural environments generally proceed sequentially from the highest energy yield downwards (Appelo & Postma, 1994). Thus, an evaluation of redox conditions in groundwater pollution plumes is often an essential prerequisite for understanding the behaviour of pollutants in the plume, and for selecting remediation approaches (Christensen *et al.*, 2000).

The study objectives for this project were to determine the groundwater redox conditions at a petroleum-contaminated site by analysing for the presence or absence of various redox species in order to make inferences about the following:

1. Whether intrinsic bioremediation of the petroleum hydrocarbons is occurring at the site and if so,
2. To determine the main redox processes responsible for the biodegradation,
3. To determine the kinetics of the redox processes, and to predict the rate of hydrocarbon degradation, and
4. To assess the limiting factors affecting biodegradation

University of Cape Town

2. SITE LOCATION AND DESCRIPTION OF THE STUDY AREA

2.1. Site location

The town of Kuils River is situated in the Western Cape province of South Africa approximately 15 km west of Stellenbosch and 23 km east of Cape Town, and overlies the Cape Flats aquifer (Figure 1.1).

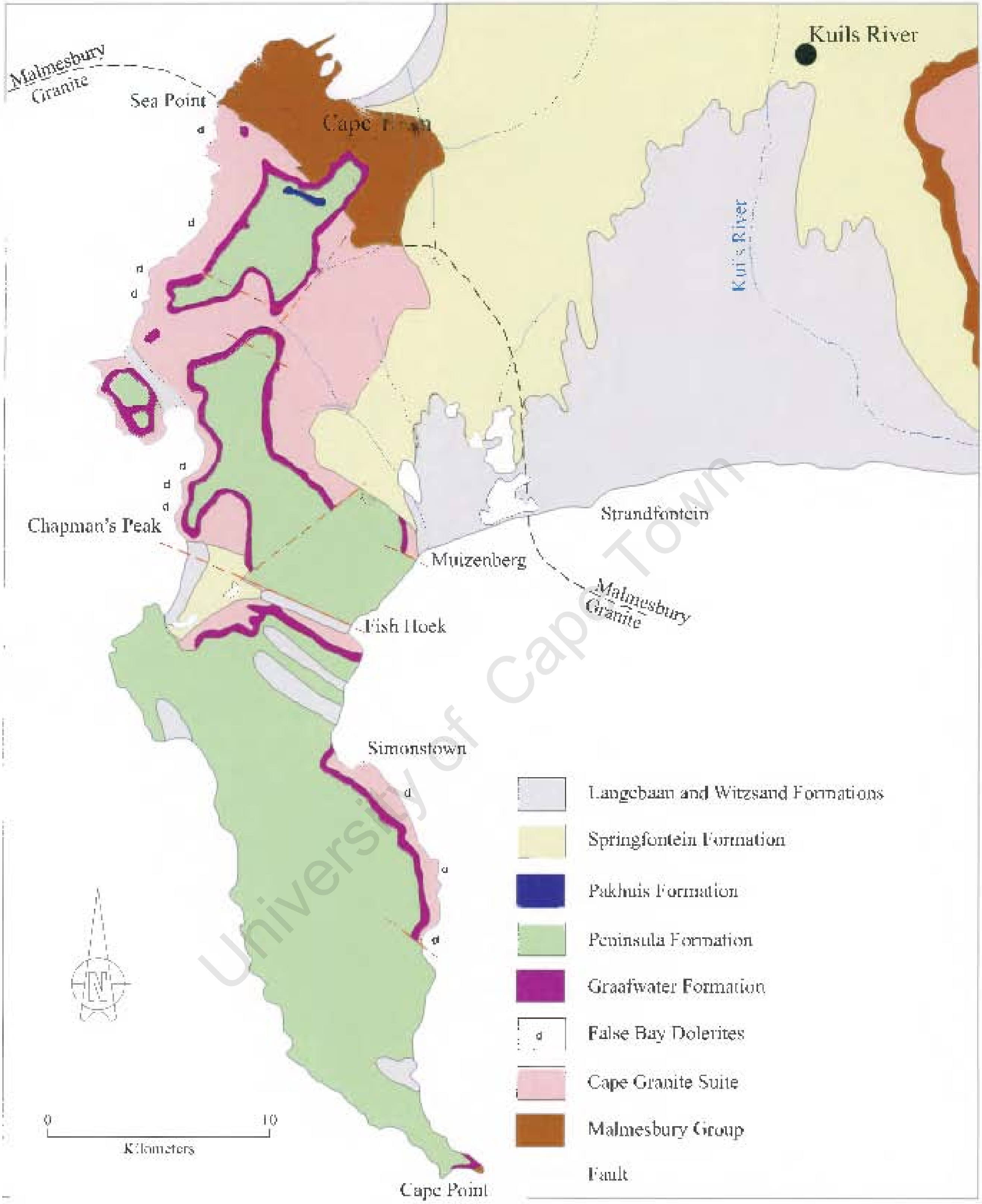

University of Cape Town

Figure 1.1. Map showing the location of Kuils River, and the geology of the Cape Peninsula within the Western Cape province of South Africa (from Reid *et al.*, 1998).

2.2. Climate

The Western Cape has a typical Mediterranean climate with hot dry summers and cold wet winters. Most of the rain falls in the winter months (May, June, July, and August) while the summers are predominantly dry. The average annual rainfall in the low flat regions to the north and east of Cape Town is 600 mm. The region experiences large geographical variations in rainfall due to the mountains which cause heavy orographic rains in places (South African Weather Bureau, 1996).

The mean temperature in summer is 21°C and in winter 13°C. Mean monthly temperatures do not vary greatly from the annual mean as a result of the moderating effect of the cool sea. The diurnal and annual temperature ranges of the inland areas are quite considerable with mean winter minimum and summer maximum temperatures varying from 2.2°C to 30.5°C (South African Weather Bureau, 1996).

The prevailing wind directions are northerly and southerly in winter, and southerly to south-easterly in summer (South African Weather Bureau, 1996).

University of Cape Town

2.3. Geology and soils

The geology of the Cape Peninsula is shown in Figure 1.1. The sandstones of the Peninsula Formation were originally linked to the same formation capping the Hottentots Holland Mountains (not shown in Figure 1.1) on the eastern fringe of the Cape Flats. Post Palaeozoic erosion has removed these sandstones between False Bay and Table Bay to create the Cape Flats (Reid *et al.*, 1998).

The oldest rocks in the area are those of the Tygerberg Formation of the Malmesbury Group. The Tygerberg Formation is predominantly composed of irregular alternations of grey to green phyllitic shale, siltstone, and medium to fine-grained greywacke. A few thin layers of lava, pyroclastics, quartzite, grit, and conglomerate are also present. Although present over a large part of the area, the rocks of this formation are covered by surficial sediments and red-brown or yellow clay (Theron, 1984). The Cape Granites (~540 Ma in age) intruded into the Malmesbury Group and forms part the Cape Peninsula Pluton of the Cape Granite Suite (Reid *et al.*, 1998). The pluton consists chiefly of a grey coarse-grained, biotite granite with large feldspar phenocrysts. The maroon sandstones and shales of the Graafwater Formation unconformably overlie the Cape Granites and form the base of the Table Mountain Group. These are overlain by the thicker bedded sandstones of the Peninsula Formation which is overlain by a remnant of the glacially deposited Pakhuis Formation (Reid *et al.*, 1998).

The Malmesbury Group and Cape Granite form the bedrock in the Cape Flats area which is overlain by the Cenozoic Sandveld Group (Reid *et al.*, 1998). Table 1.1 shows the stratigraphy of the Sandveld Group.

For the purpose of this thesis, only the Quaternary aged sediments will be described in any detail as these form the sediments of the Cape Flats. The surficial soils in the Kuils River area were formed *in situ* on the Malmesbury rocks during weathering. The soil formed is yellow, red, or brown. It is clayey and frequently contains small nodules of ferricrete and fragments of vein quartz, in addition to a variable quantity of sand grains (Theron *et al.*, 1992). The estimated thickness of the soil and depth to the bedrock is estimated to be about 10 m (Van der Merwe, 2000).

University of Cape Town

Table 1.1. Cenozoic Formations of the Western Cape (from Theron *et al.*, 1992).

Age			Lithology	Formation	
Quaternary	Holocene		Aeolian, calcareous, quartzose sand	Witzand	Sandveld Group
	Pleistocene		Aeolian, calcrete-capped calcareous sandstone	Langebaan	
			Littoral, calcrete-capped coquina	Velddrif	
			Fluvial gravel, marine clay and littoral sand	Milnerton	
			Aeolian, quartzose sand with intermittent peaty layers	Springfontein	
Neogene	Pliocene		Quartzose and muddy sand, and shelly gravel, phosphate-rich	Varswater	
	Miocene	Late	Conglomeratic sandy phosphorite	Saldanha	
		Middle	Angular quartzose gravely sand and peaty clays	Elandsfontyn	

University of Cape Town

2.4. Geohydrology

The hydrogeology of the different geological units in the south-western Cape has been divided into: fractured aquifers, fractured and intergranular aquifers, and intergranular aquifers (Meyer, 2000). The Cape Flats Aquifer, on which the site under investigation is situated, is one of the most extensive sand aquifers in South Africa (Meyer, 2000). It is an intergranular aquifer which is defined by Meyer (2000) as generally unconsolidated but occasionally semi-consolidated, and groundwater occurs within intergranular interstices in a porous medium. The typical yields from boreholes in the area are in the range from 0.1 to 0.5 $L.s^{-1}$. Other properties of the Cape Flats aquifer groundwater are given in Table 1.2.

Locally the groundwater occurs at a depth of 2.5 to 3.0 m below the surface but fluctuations in the depth of the water table occur on a seasonal basis. The Kuils River itself is approximately 1 km away from the site in a south-westerly direction which is also the direction of the hydraulic gradient (Van der Merwe, 2000).

Table 1.2. Hydrogeological properties of the Cape Flats aquifer (from Meyer, 2000).

EC (mS/m)	Potential groundwater yield ($10^6 m^3/a$)	Transmissivity (m^2/day)	Recharge (%)*	Storage ($10^6 m^3$)	Mean annual precipitation (mm)
60 – 135	15	250 – 600	15 – 35	1500	91

* % of the mean annual precipitation

University of Cape Town

2.5. Site description

2.5.1. Land use

The site currently serves as an Engen petrol station, and the Kuilsriver Toyota dealer consisting of a vehicle showroom, spare parts, storage/sales facilities, and a workshop. The land is used for various purposes in the immediate vicinity of the site. Opposite the station, to the east (Van Riebeck Street), there is a residential area consisting of apartment buildings. To the west and south of the site, Industry Road and Energy Road respectively, the land is used for commercial purposes, while a police station and magistrates court exists to the north of the area.

2.5.2. History of contamination and remedial actions taken

Between the period from the 8th to the 18th September 2000, there was a leak from a 14 m^3 underground storage tank used for the storage of 97-octane petrol (Van der Merwe, 2000). During this period a volume of 101560 L leaked from a hole, located underneath the storage tank, into the surrounding groundwater system. In order to monitor the spread of the free phase product (FPP) plume and dissolved hydrocarbons, a total of 45 PVC-cased monitoring wells were put in place (Figure 1.2). The initial assessment of the contamination showed that the FPP floating on top of the groundwater reached a maximum thickness of 1000 mm in places. Product recovery from 24 of the monitoring wells commenced using vacuum-enhanced extraction. Subsequent dipping of the monitoring wells revealed that the thickness of the FPP had been reduced substantially and it was therefore recommended that recovery of the FPP be continued. As at 22nd March 2001, a total of 82340 L (81 % of the reported leakage) of the free phase product had been removed using vacuum-enhanced extraction (McBride, 2001). The extracted fuel and contaminated water was disposed of at Vissershok hazardous waste disposal site and/or Fuel Firing Systems. During April 2001, further vacuum extraction was attempted but no significant additional volumes of the FPP were recovered. Use of the 14 m^3 storage tank ceased and two new 23 m^3 underground storage tanks were installed.

University of Cape Town

Groundwater samples from various wells were analysed for BTEX. The concentrations of benzene in groundwater sampled from GM9 (Figure 1.2) on the 12th November 2001 were found to be 119000 µg/L (Mcbride, 2001). This is unusually high as analyses carried out on water samples from the same well before and after this date were between 16000 and 26000 µg/L. These concentrations pose an unacceptable risk to human health as benzene

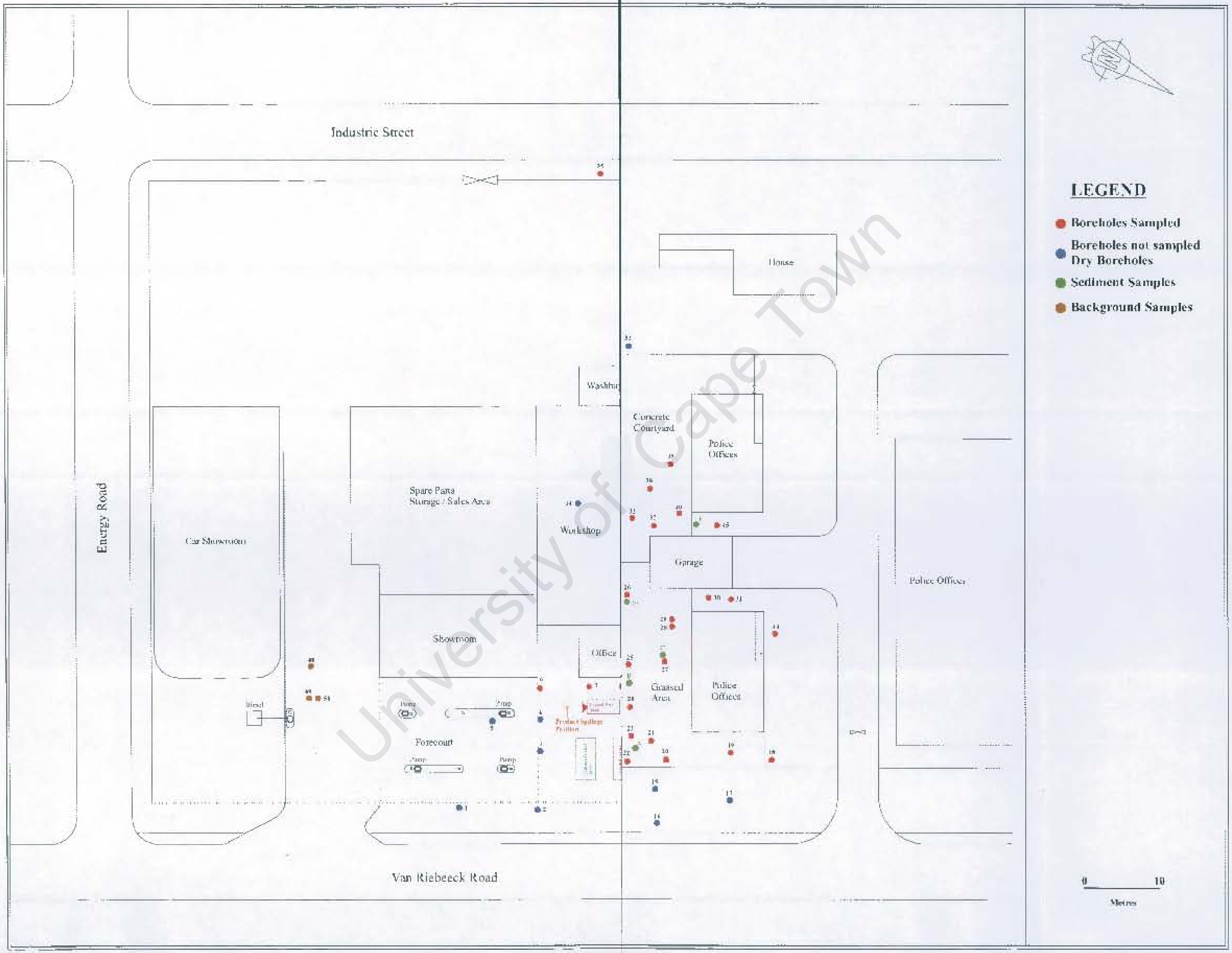

University of Cape Town

Figure 1.2. Site layout showing the location of sampled boreholes and sediments.

vapours entering buildings from groundwater are likely to result in elevated cancer risk to residents. Use of the houses adjacent to the site as housing for the South African Police was discontinued. The houses are currently being used as offices. There are no groundwater abstractions or open bodies of water in the area and ingestion of groundwater is therefore considered unlikely. Appendix A shows an aerial photograph of the site.

3. REDOX PROCESSES IN CONTAMINATED AQUIFERS: A LITERATURE REVIEW

3.1. Theory

3.1.1. Electron activity (pε)

University of Cape Town

Aqueous solutions do not contain free electrons (Stumm & Morgan, 1996). The redox intensity parameter pε gives the electron activity at equilibrium, and measures the tendency of a system to accept or transfer electrons. The pε is defined as:

$$p\varepsilon = -\log \{e^-\}$$

A solution that is highly reducing has a tendency to donate electrons i.e. the electron activity is relatively large and therefore the electron activity is very low at high pε. A high pε thus indicates a relatively high tendency for oxidation.

For any reduction reaction, an oxidised species Ox reacts with *n* electrons to form a reduced species Red, and can be written as:

$$Ox + ne^{-} \rightarrow Red$$

For this reaction, the equilibrium constant K is defined as:

$$K = \{Red\}/\{Ox\}e^{-n}$$

This leads to:

$$p\varepsilon = (1 / n) \log K + (1 / n) \log [\{Ox\}/\{Red\}]$$

Since there are no free electrons in a system, the reduction reaction must therefore be linked to an oxidation reaction. For reference purposes the oxidation of hydrogen is used which leads to the following equation:

$$p\varepsilon = p\varepsilon^{0} + (1 / n) \log [\{Ox\}/\{Red\}]$$

In the equation above, $p\varepsilon^{0}$ is the standard electrode activity of the net or overall redox reaction when coupled to the oxidation of hydrogen under standard conditions.

3.1.2. Redox potential (E_h)

The electron activity is, via the Nernst equation, linked to the redox potential (E_h) (Christensen, *et al.,* 2000):

$$E_h = p\varepsilon \left(\frac{2.3RT}{F}\right)$$

or:

University of Cape Town

$$E_h = E_h^0 + (2.3\,RT / nF) \log [\{Ox\}/\{Red\}]$$

T is the absolute temperature (in Kelvin), *R* is the gas constant (8.3145 $J.mol^{-1}.K^{-1}$), and F is Faraday's number (96485 C / mol e^-).

3.1.3. Problems associated with direct Eh measurements

Laboratory studies have yielded Eh measurements that are in agreement with the Nernst equation. However, the redox processes observed in natural waters are generally not at equilibrium, and the redox potentials are mixed potentials which are impossible to relate to a single dominant redox couple in solution (Lindberg & Runnells, 1984). Figure 1.3 shows the Eh values measured in the field with those calculated using the Nernst equation. The lack of agreement between the data points shows that internal equilibrium is not achieved. It is noted that factors such as delays in sample chemical analyses and inadequate sample preservation affect the values. The usefulness of Eh measurements as a qualititative indicator of the overall redox state is noted.

Chapelle *et al.* (1996) noted that the size of the Fe (III) reducing zone in an aquifer was overestimated. A possible explanation given for this is that Fe^{3+} and Fe^{2+} are highly electroactive on platinum electrodes.

University of Cape Town

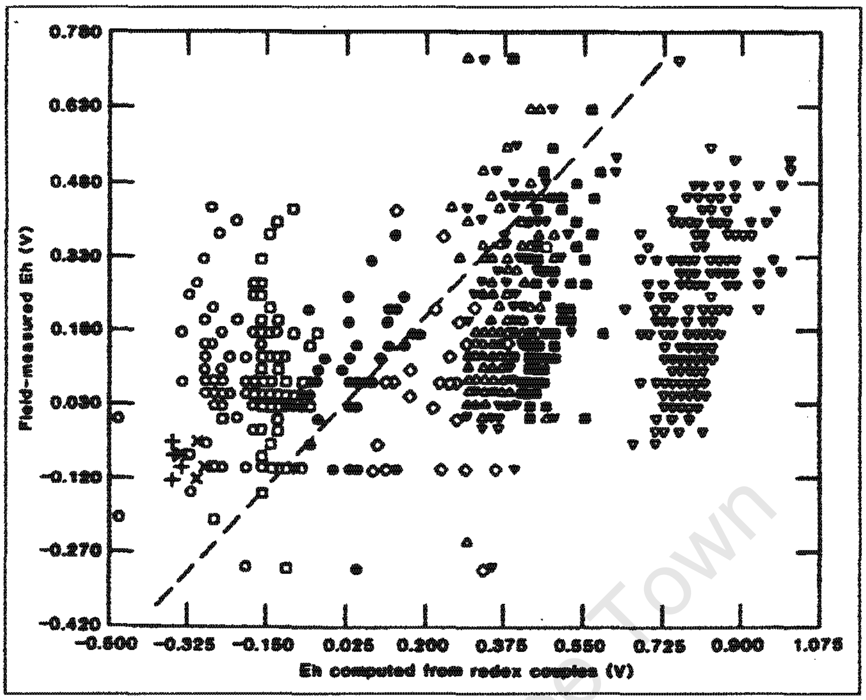

Figure 1.3. Plot of field measured Eh values versus computed Nernstian Eh values. The symbols represent the following redox couples: ◊ Fe^{3+}/Fe^{2+}, ∇ $O_{2\,aq}/H_2O$, O HS^-/SO_4^{2-}, □ $HS^-/S_{rhombic}$, ■ NO_2^-/NO_3^-, ▼ NH_4^+/NO_3^-, Δ NH_4^+/NO_2^-, + $CH_{4\,aq}/HCO_3^-$, x $NH_4^+/N_{2\,aq}$, • $Fe^{2+}/Fe(OH)_{3\,(s)}$ (from Lindberg & Runnells, 1984).

University of Cape Town

3.2. Microbial mediation of redox processes and redox zonation

The role that bacteria play in reducing inorganic terminal electron acceptors (such as SO_4^{2-}, NO_3^-, Fe^{3+} etc) in anoxic or reducing environments has been documented by many authors (Baedecker & Back, 1979; Cazzarelli *et al.*, 1999; Cozzarelli *et al.*, 2001; Jackobsen & Postma, 1999; Lovley & Goodwin, 1988; Ludvigsen *et al.*, 1998). Bacteria act only as catalysts and therefore do not oxidise substrates or reduce terminal electron acceptors such as O_2 or SO_4^{2-} (Stumm & Morgan, 1996). Redox processes proceed sequentially from the highest energy yield downward (Appelo & Postma, 1994; Postma & Jackobsen, 1996). Data for the energy yield from the oxidation of natural organic matter by various inorganic TEA's the synthesis of new cells, and for maintaining old cells (Stumm & Morgan, 1996). The groundwater habitat of the microbes must provide the soluble nutrients for the synthesis of nutrients (Champ *et al.*, 1979). Figure 1.4 shows the typical sequence of microbially mediated redox processes. Figure 1.5 shows the changes in the concentrations of some of the reactants and products of redox reactions.

Table 1.3. Gibb's energy of reaction calculated for the oxidation of organic carbon by various electron acceptors and by methane fermentation of organic carbon (from Christensen *et al.*, 2000).

Process	Reaction	ΔG^0 (W) [a] [kJ eq^{-1}]
Aerobic respiration	$\frac{1}{4}\ CH_2O + \frac{1}{4}\ O_2 \rightarrow \frac{1}{4}\ CO_2 + \frac{1}{4}\ H_2O$	-125
Denitrification	$\frac{1}{4}\ CH_2O + \frac{1}{5}\ NO_3^- + \frac{1}{5}\ H^+ \rightarrow \frac{1}{4}\ CO_2 + \frac{1}{10}\ N_2 + \frac{1}{2}\ H_2O$	-119
Mn reduction	$\frac{1}{4}\ CH_2O + \frac{1}{2}\ MnO_2 + \frac{1}{2}\ HCO_3^- + \frac{1}{2}\ H^+ \rightarrow \frac{1}{4}\ CO_2 + \frac{1}{2}\ MnCO_3 + \frac{3}{4}\ H_2O$	-98
Fe reduction	$\frac{1}{4}\ CH_2O + FeOOH + HCO_3^- + H^+ \rightarrow \frac{1}{4}\ CO_2 + FeCO_3 + \frac{7}{4}\ H_2O$	-42
SO_4^{2-} reduction	$\frac{1}{4}\ CH_2O + \frac{1}{8}\ SO_4^{2-} + \frac{1}{8}\ H^+ \rightarrow \frac{1}{4}\ CO_2 + \frac{1}{8}\ HS^- + \frac{1}{4}\ H_2O$	-25
CO_2 reduction / methane fermentation	$\frac{1}{4}\ CH_2O \rightarrow \frac{1}{8}\ CO_2 + \frac{1}{8}\ CH_4$	-23

[a] Standard Gibb's free energy of reaction in neutral water (pH = 7.0) at 25°C.

University of Cape Town

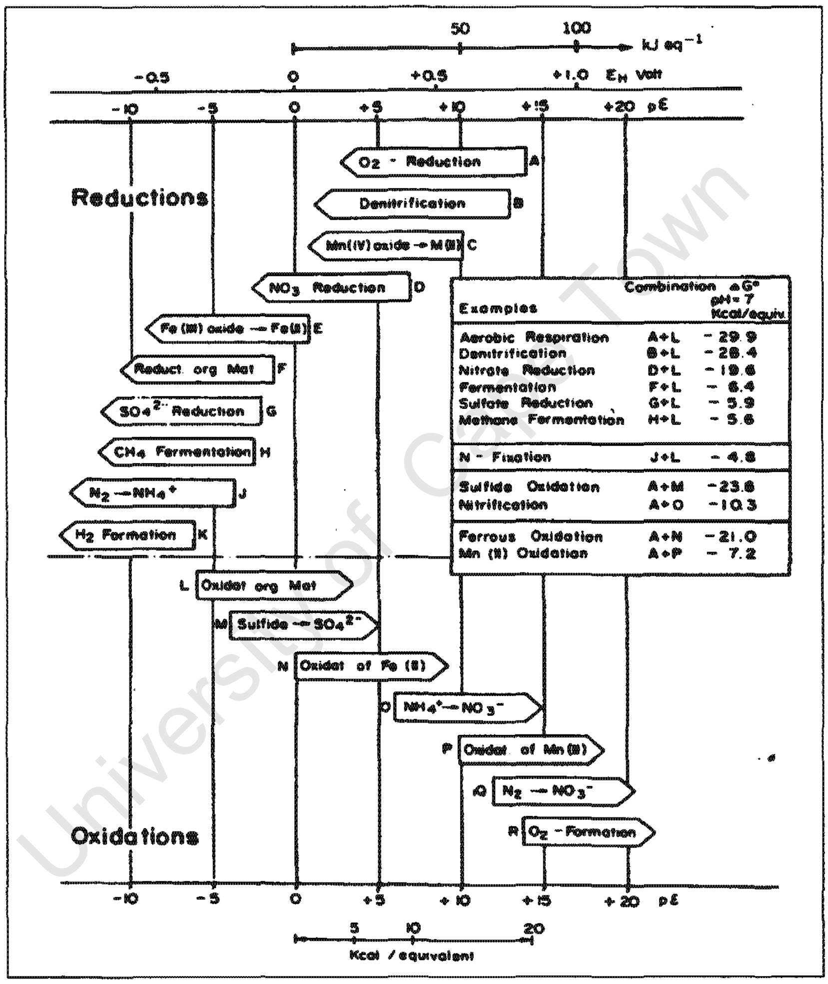

Figure 1.4. Sequence of microbially mediated redox reactions (from Stumm & Morgan, 1996).

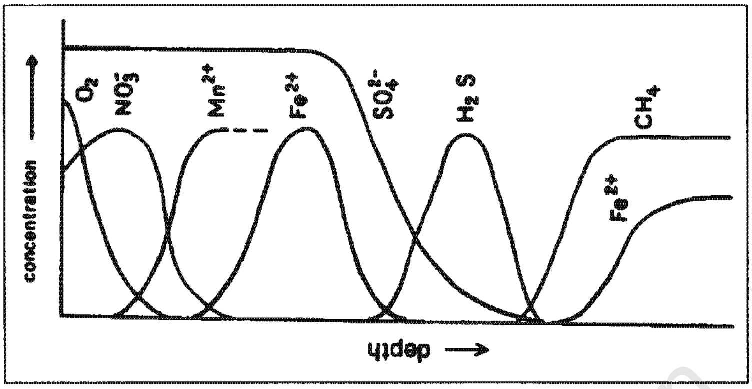

Figure 1.5. Variation in groundwater chemical composition as redox reduction processes take place (from Appelo & Postma, 1994).

3.3. Redox zones in contamination plumes

The concept of redox zonation is not new and has been reported by many authors (Champ *et al.*, 1979; Lyngkilde & Christensen, 1992; Bjerg *et al.*, 1995; Postma & Jackobsen, 1996; Norkus *et al.*, 1996; Ludvigsen *et al.*, 1998). The identification of the various redox zones at contaminated sites is based on the concentrations of the products or reactants of the various redox processes. Intrinsic bioremediation is indicated by the depletion of oxygen, nitrate, and sulphate within the contaminant plume, as well as the production of dissolved CO_2 and Fe^{2+} (Borden *et al.*, 1995). The observed sequence of various redox reactions also depends on the availability of the various TEA's. If some of these electron acceptors are missing, then the corresponding redox zones are also missing (Lyngkilde & Christensen, 1992). Lovley and Goodwin (1988) noted that once Fe (III) reduction became limited by Fe (III) availability, Fe (III) reducers were no longer able to out compete sulphate reducers for

University of Cape Town

electron donors. Once the TEA's are consumed, the rate of biodegradation slows considerably (Borden *et al.*, 1995).

Although Champ *et al.* (1979) did not distinguish between all of the redox zones known to be found, they did recognise the fact that variations in the Eh of an aquifer could be accounted for by a sequence of redox reactions occurring in the flow systems. They concluded that 3 zones could be identified. As dissolved organic carbon (DOC) reduces oxygen and nitrate, a more reducing environment is produced in which iron and manganese reduction occurs. After the reduction of iron and manganese, sulphate reducing bacteria reduce sulphate to sulphide. Other authors (Norkus *et al.*, 1996) have not distinguished between the various redox zones, and only used certain parameters to delineate an aerobic zone, a transitional zone, and an anaerobic zone.

The study of redox zonation has come a long way since the early work done by many authors. The redox zone sequence observed in the study carried out on a landfill leachate pollution plume by Lyngkilde and Christensen (1992) was consistent with thermodynamic principles. One of the points highlighted in the study is that the determination of an exact redox potential is not needed in order to identify the various redox zones. Instead, the identification of dominating redox process is the determining factor that leads to the assignment of redox status in an aquifer (Table 1.4). The delineation of redox process into specific zones is also complicated by the fact that several redox processes maybe taking place in the same area and thus areas of overlap or transition areas occur (Bjerg *et al.*, 1995; Ludvigsen *et al.*, 1998).

University of Cape Town

Table 1.4. Criteria for redox parameters used for assigning redox status to groundwater samples. All values expressed as $mg.L^{-1}$ (from Lyngkilde & Christensen, 1992).

Parameter	Aerobic	Nitrate reducing	Manganogenic	Ferrogenic	Sulfidogenic	Methanogenic
Oxygen	> 1.0	< 1.0	< 1.0	< 1.0	< 1.0	< 1.0
Nitrate	*	*	< 0.2	< 0.2	< 0.2	< 0.2
Nitrite	< 0.1	*	< 0.1	< 0.1	< 0.1	< 0.1
Ammonium	< 1.0	*	*	*	*	*
Mn (II)	< 0.2	< 0.2	> 0.2	*	*	*
Fe (II)	< 1.5	< 1.5	< 1.5	> 1.5	*	*
Sulphate	*	*	*	*	*	< 40
Sulphide	< 0.1	< 0.1	< 0.1	< 0.1	> 0.2	*
Methane	< 1.0	< 1.0	< 1.0	< 1.0	< 1.0	> 1.0

* = no criterion is applied

3.4. Aerobic biodegradation

Almost all hydrocarbons are biodegradable under aerobic conditions (Borden *et al.*, 1995). However, the low solubility of oxygen in water is a limiting factor for the aerobic biodegradation in the subsurface.

3.5. Nitrate, nitrite, ammonia, and nitrogen

Nitrate accepts electrons from reduced carbon sources. This leads to the formation of reduced compounds such as nitrogen gas (denitrification) and ammonium (dissimilatory nitrate reduction) according to the following reactions (Norkus *et al.*, 1996):

$$86\ NO_3^- + 12\ C_7H_8 \rightarrow 43\ N_2 + 84\ HCO_3^- + 6\ H_2O \text{ (denitrification)}$$

$$91\ H^+ + 22\ NO_3^- + 3\ C_7H_8 \rightarrow 22\ NH_4^+ + 21\ HCO_3^- + 3\ H_2O \text{ (dissimilatory reduction)}$$

University of Cape Town

Norkus *et al.* (1996), through the use of nitrate and ammonia electrodes, were able to establish that nitrate reduction at a gasoline contaminated site occurred via the dissimilatory reduction to ammonia. Other studies have used the measured concentrations of nitrate and ammonium as evidence for nitrate reduction are those carried out by: Lyngkilde and Christensen (1992); and Bjerg *et al.*, (1995).

The products of denitrification can be either N_2 or N_2O (Ludvigsen *et al.*, 1998). N_2O is a product of the oxidation of ammonia and may occur in a narrow zone near the water table where O_2 is available (Cozzarelli *et al.*, 1999). In more oxidised environments denitrification may be favoured. The determination of the dominant nitrate reducing mechanism is complicated as there are multiple possible sources and sinks for ammonia (Cozzarelli *et al.*, 1999).

3.6. Iron and sulphate reduction

Fe (III) oxides are abundant in most sand and gravel aquifers but variations in the distribution of sedimentary iron may be heterogeneous, and the scale of the heterogeneity may vary as well (Cozzarelli *et al.*, 2001). Sediment geochemistry is integral to Fe (III) reduction as the source of Fe (III) that is reduced is mainly Fe (III)-bearing minerals (Tuccillo *et al.*, 1999).

In the study by Cozzarelli *et al.* (2001) microbial iron reduction and precipitation, sorption and/or oxidation of Fe^{2+} is found to control the movement of the dissolved iron plume. Fe (III) is depleted in the anoxic zones, and accumulates in the oxic zone, and in the

University of Cape Town

oxic/anoxic transition zone. It was also found that methanogenesis occurs concurrently with iron reduction.

Tuccillo *et al.* (1999) showed that microbial reduction of crystalline iron oxides is possible in a contaminated aquifer. Some of the reduced Fe is then stored in the sediments as Fe (II) bearing minerals or as organically bound Fe. Pyrite (FeS_2) and marcasite (FeS) are two of the most abundant iron sulphide minerals found (Appelo & Postma, 1994). The formation of pyrite in sediments is reported to be a two step process:

$$\text{Step 1: } 2FeOOH + 3HS^- \rightarrow 2FeS + S^o + H_2O + 3OH^-$$

$$\text{Step 2: } FeS + S^o \rightarrow FeS_2$$

The sequential occurrence of Mn (IV), Fe (III), SO_4^{2-} reduction and methanogenesis is explained more easily by the partial equilibrium approach where the fermentative step is overall rate limiting, and the electron accepting processes are considered to be close to equilibrium. Depending on the stability of the iron oxide, simultaneous reduction of Fe (III) and sulphate is thermodynamically possible under a wide range of sedimentary conditions. In Fe^{2+} rich environments the pH of porewater has a strong influence on whether Fe (III) or sulphate reduction is favoured (Postma & Jakobsen, 1996).

Bjerg *et al.* (1995) found that where high sulphide concentrations were detected, low sulphate concentrations were found.

University of Cape Town

3.7. pH

The pH has also been observed to change as a contaminant plume evolves. Champ *et al.* (1979) noticed that a decrease in the Eh was accompanied by an increase in the pH. The increase in pH was attributed not only to the dissolution of calcite, but also due to other processes such as ion exchange, adsorption, and hydrolysis of silicate minerals. The study carried out by Cozzarelli *et al.* (1999) shows that uncontaminated background water samples had pH measurements of about 4.73, while the pH was near neutral nearer the central parts of the contaminant plume.

University of Cape Town

4. THE SIGNIFICANCE OF GEOLOGICAL HETEROGENEITIES

4.1. The impact of aquifer sediment grain size on hydrocarbon distribution

Aelion (1996) conducted a study on coastal plain sediments consisting of unconsolidated, fine-grained sands, with inerfingering lenses of clay. A grain size analysis of the sediments was performed and all sediments were analysed for BTEX. The results of the investigation show that jet fuel contamination was positively correlated with the clay content of the sediments. Two sediment samples, collected from a single borehole, with the greatest difference in clay content of the contiguous samples collected, were used for microcosm experiments. One was predominantly clay and the other predominantly fine sand. Results indicate that bacteria in the sandy sediment were more active than those in the clay sediment. Amino acids, toluene, and benzene were mineralised to a greater extent in the sandy sediments. Factors other than the clay content may be responsible for the observed differences in microbial activity. It is suggested that in a bioremediation system, sandy sediments will be more readily remediated due to preferential flow through the sandy sediments.

Similar results were found in a study carried out by Cozzarelli *et al.* (1999) on a coastal plain aquifer contaminated by a gasoline spill. It was found that anaerobic processes were dominant in a clay unit with low permeability, while nitrate reduction and aerobic degradation occurred in the permeable sandy layers. The study also showed that hydrocarbons were more persistent over time in the low permeability clay horizon. The explanation given for this is that the hydrocarbons are trapped to some degree in the clay horizon, and that there is a limited availability of electron acceptors for degradation. This is as a result of the low permeability of the clay unit. The perched water table that has developed above the clay horizon, in the sandy sediments, is supplied by vertical recharge from precipitation events that supply oxygen, NO_3^-, and SO_4^{2-}. The low permeability of the clay unit limits the supply of electron acceptors.

4.2. Sediment characterisation

Sediment plume characterisation is recommended in all plume investigations and past investigations have mainly been focused on iron and sulphur compounds (Christensen *et al.*, 2000). This is because analytical distinction between Mn (IV) and Mn (II) is difficult. Heron *et al.* (1998) have demonstrated the need for a small-scale geological model and detailed mapping of sediment geochemistry. Without such a model, it is difficult to distinguish between the impacts caused by the contaminant plume from the natural variations in aquifer geochemistry. This is demonstrated by the occurrence of a thin layer at the study site which

University of Cape Town

is dominantly silt and clay. This layer was found to be rich in organic matter and has a high iron content. It is noted that such a layer may be naturally anaerobic and Fe (II) rich.

University of Cape Town

CHAPTER 2 - METHODOLOGY

1. GROUNDWATER SAMPLE COLLECTION AND ANALYSIS

The sampling strategy that was employed throughout the duration of the project was designed in order to be as cost-effective and simple as possible. Sample collection took place during September 2003 and was a once-off event. As a result of the time constraints placed on the project, additional sample collection was not possible. Ideally, several seasonal sampling events should be planned in order to assess the temporal variation in groundwater chemistry which can provide an indication of the variability of intrinsic bioremediation.

1.1. Field measurements and sample collection procedure

Groundwater samples were collected from thirty-two wells that are cased with slotted PVC pipes and capped. The location of the wells is illustrated in Figure 1.2. Three wells (GM48, GM49, and GM50) are located up-gradient of the spillage position and serve as background samples. To obtain a groundwater sample that is representative of conditions at the site, all wells were purged of approximately three well volumes. Effective well purging was carried out using a pump, and in some cases where there was very little water present in the well Teflon bailers were used. After each purge, measurements of pH, electrical conductivity, dissolved oxygen, and temperature were made using a WTW Multi 340i Set. Eh was measured using a Sentek portable Eh electrode. Purging continued until the Eh, electrical conductivity, and temperature stabilised. The functioning of each electrode was verified by calibrating the instrument prior to commencing field work each day, and at random time intervals while in the field.

University of Cape Town

Groundwater samples were collected using Teflon bailers. To minimise the introduction of oxygen into the groundwater, the bailer was lowered gently in such a manner to minimise splashing, and thus the introduction of oxygen into the sample. The bailer was removed and the samples were poured into an Erlenmeyer flask to measure the above mentioned field parameters.

Samples of each well were also collected in 250 ml plastic bottles that were filled to the top in order to minimise the amount of oxygen trapped in the headspace once the bottles were capped. Each plastic bottle was thoroughly rinsed with the sample before filling the bottles. After returning from the field each day, these samples were then filtered using a 0.45 µm filter. Approximately 100 ml of the sample was filtered and used to fill two 50 ml VWR brand centrifuge tubes to the top. No additives or preservatives were added to the sample in the first tube. This was used for the determination of anions as described in section 1.3.5 below. The sample in the second tube was acidified using concentrated HCl to a pH < 2 for the determination of major cations (see section 1.3.6.). Until the analyses were carried out, the samples were stored as described below.

University of Cape Town

1.2. Sample storage and transportation

While in the field, all samples were stored under anoxic conditions by placing the samples into an anoxic chamber. An anaerobic atmosphere was maintained in the chamber by placing Merck Anaerocult® A pills into the chamber to which de-ionised water was added. This was repeated each time the anaerobic chamber was opened to place a new sample inside. The chamber was kept cool by placing the chamber into a cooler filled with ice packs. On returning from the field each day, the samples were placed into a plastic bag that was flushed with nitrogen, which was sealed and placed into a second nitrogen filled bag. The bags were then placed in a refrigerator until required for analysis.

1.3. Analytical techniques

1.3.1. Determination of Fe^{2+}

The ferrozine method modified after Stookey (1970) was used to determine the concentrations of Fe^{2+} in the samples. The ferrozine buffer was prepared by weighing out approximately 0.2 g ferrozine and 12 g of Hepes. These were then placed into a 1 L volumetric flask and made up to 1 L using de-ionised water. The pH of the ferrozine buffer was adjusted to pH of 7 using 10 M NaOH. A 0.01 M ferrous sulphate ($FeSO_4.7H_2O$) stock solution was prepared. In order to prevent the iron (II) from oxidising and precipitating, a few mL of concentrated HCl was added. In order to prepare standards for the calibration curve, dilutions of the stock solution were made.

Sample collection was done using a syringe that was flushed with the sample prior to filtering. Sufficient sample for the determination of Fe^{2+}, alkalinity (see section 1.3.2), and sulphide (see section 1.3.3) was then filtered through a 0.45 µm filter into a beaker. Using an auto pipette, 250 µL of the filtered sample was pipetted into 15 mL VWR Brand centrifuge tubes that were charged with 5 mL of ferrozine in order to fix Fe^{2+}.

In order to determine the concentration of Fe^{2+}, the absorbance of the samples and standards was measured at 562 nm using a spectrophotometer. The concentrations were then determined from the calibration curve which is determined by linear regression analysis of the standards. A new calibration curve was prepared each day.

1.3.2. Determination of alkalinity

The method of Sarazin *et al.* (1999) was used for the determination of alkalinity. This method employed measures the total alkalinity and not only the carbonate alkalinity (Sarazin *et al.*, 1999).

Alkalinity standards were prepared by making dilutions of a 0.1 M $NaHCO_3$ stock solution. The colour reagent is prepared by mixing 25 mL of 0.1 M formic acid and 25 mL of a solution of Bromophenol-Blue (500 mg.L^{-1}) in 250 mL volumetric flask.

While in the field, 2 mL of filtered sample was pipetted into 15 mL VWR Brand centrifuge tubes that contained 2 mL of the colour reagent. This was also done for the standards that were prepared. The absorbance of the standards and samples was measured at 590 nm using a spectrophotometer on returning form the field each day. The alkalinity of the samples is then determined by fitting a second order polynomial function to the standards which allows the alkalinity of the samples to be calculated.

1.3.3. Determination of sulphide

5 mL of the filtered sample mentioned in section 1.3.1 above was pipetted into a 15 mL VWR brand centrifuge tube. Five drops of a 20 % (w/v) zinc acetate solution was added in order to trap the sulphide. To this, about 40 µL of 6 M NaOH was added to raise the pH of the sample to 8. The samples were stored as described in section 1.2 above, until the

University of Cape Town

analysis was carried out using the method of Cline (1969). This is due to the fact that it is recommended that fresh standards be made up every day, and the process is quite time consuming.

Mixed diamine reagent was prepared for a sulphide concentration in the range of 3 to 40 µM. This is done by dissolving 2 g of N,N-dimethyl-p-phenylenediamine sulphate and 3 g ferric chloride ($FeCl_3.6H_2O$) in 500 mL of cool 50 % (v/v) reagent grade HCl.

The preparation of standards was done as follows. Oxygen free water was prepared by purging 2 L of de-ionised water with nitrogen for 1 hour. Using this, a 0.01 M $Na_2S.9H_2O$ stock solution was the prepared. The standards were then prepared by making dilutions of the stock solution with the nitrogen purged de-ionised water.

For the determination of sulphide, the samples preserved with zinc acetate were shaken thoroughly, and 3 mL of the sample pipetted into a 15 mL VWR Brand centrifuge tube. 0.4 mL of the mixed diamine reagent was then added to this. After 20 minutes, the absorbance was determined spectrophotometrically at 670 nm. The sulphide concentration of the sample is then calculated from the calibration curve.

1.3.4. Determination of NH_4^+

Ammonium standards were made up by making dilutions of a 0.1 M NH_4Cl stock solution. The method of (Solorzano, 1969) was used and is described below.

University of Cape Town

The following reagents were made:

- Phenol solution – Made by dissolving 10 g of crystalline analytical reagent grade phenol in 100 ml of 95 % v/v ethanol.
- Sodium nitroprusside solution – Dissolved 0.5 g sodium nitroprusside in 100 mL de-ionised water
- Alkaline reagent – 50 g of sodium citrate, and 2.5 g of sodium hydroxide were dissolved in 250 mL of de-ionised water
- Sodium hypochlorite solution – Household bleach (JIK). This is a solution of 3.5 % (m/v) sodium hypochlorite.
- Oxidizing solution - This is prepared by mixing 100 mL of the alkaline reagent and 25 mL of the sodium hypochlorite solution.

3 mL of sample or standard was added to a 15 mL VWR Brand centrifuge tube, and the phenol solution was added by pipetting 120 µL. The solution was then mixed thoroughly using a Vortex Genie. Then 120 µL of the sodium nitroprusside solution and 300 µL of the oxidising solution were sequentially added, mixing after each addition using the Vortex Genie. The centrifuge tubes were covered with aluminium foil, capped, and then allowed to stand at room temperature for 1 hour for full colour development. The absorbance of the samples and standards was then measured at 640 nm. The concentration of the samples was determined from the calibration curve. The measured absorbance was corrected using a reagent blank. In some cases, the measured absorbance was higher than the standard of the highest concentration. Samples were then diluted and reagents were added in the same proportions as described above. The final concentrations were then calculated by taking the dilution factor into account.

University of Cape Town

1.3.5. Determination of SO_4^{2-} and NO_3^-

The concentrations of SO_4^{2-} and NO_3^-, as well as Cl^-, F^-, and Br^-, was determined on samples that had been filtered in the lab using a 0.45 µm filter and stored in a 50 mL centrifuge tube as described in section 1.1. All samples were kept cool in a fridge until analysis was carried out. Samples were analysed using a Dionex Ion Chromotography in the Department of Geological Sciences at the University of Cape Town.

1.3.6. Major cations

The determination of Fe, Mn, Na, K, Ca, and Mg was done using Atomic Absorption Spectrometry in the Department of Chemical Engineering at the University of Cape Town. All samples analysed in this manner were filtered in the lab using a 0.45 µm, and acidified to a pH < 2 using concentrated HCl. Samples were stored in a fridge until the analysis was carried out.

University of Cape Town

2. Sediment Collection and Analysis

2.1. Sediment sampling procedure

Sediment sampling was done using an auger to penetrate down to a depth of approximately 2.5 m. This was generally the depth at about which the groundwater was reached. Shortly before encountering the groundwater, a strong smell of petroleum was always detected emanating from the holes. The samples were double-bagged in polyethylene sampling bags. As much air as possible was forced out of the bags and they were tightly sealed.

2.2. Iron oxide extractions

Single step extractions of various mineral phases were performed using the following leachates:

- Ascorbate solution (pH = 8) – This is prepared by adding 5 g ascorbic acid, 12.5 g of sodium citrate, and 12.5 g of sodium bicarbonate in 250 mL deionised water.
- Buffered sodium dithionite (pH = 4.8) – Prepared by making an acetic acid buffer solution of 0.35 M, in which the concentration of sodium citrate is 0.2 M. Then 0.5 g of sodium dithionite is added per 10 mL of the buffer solution.

The ascorbate solution extracts amorphous iron oxyhydroxides and minor iron associated with acid volatile sulphides (AVS), while buffered sodium dithionite completely extracts all of the reactive iron oxides except magnetite.

Pre-weighed samples of the sediment were placed in 15 mL VWR Brand centrifuge tubes containing 10 mL aliquots of the leachate, and placed on a shaker at 125 rpm. The tubes containing buffered sodium dithionite and ascorbate solution were shaken for 2 and 24 hours respectively. After shaking, the tubes were centrifuged at 5000 rpm for 5 minutes. The supernatant was decanted off and filtered using a 0.45 µm filter, and 8 mL of the filtered sample was acidified to a pH < 2 using concentrated HCl.

University of Cape Town

The total iron concentration of the samples was determined colourimetrically using the ferrozine method. 100 µL of the sample was pipetted into 5 mL of ferrozine reductant and the absorbance measured using a Sequoia Turner Corporation model 340 spectrophotometer.

2.3. Incubation experiments

Incubation experiments were carried out in order to determine the change in Fe^{2+} and SO_4^{2-} concentrations over time to determine the rates of iron and sulphate reduction. Sediments from three sites: GM13, GM26, and GM27, was used to carry out incubation experiments. Each sample was homogenised inside an anaerobic chamber using a spatula, and the sediment slurries used to fill fourteen 50 mL VWR Brand centrifuge tubes. The centrifuge tubes were then capped and kept at the ambient temperature inside the anaerobic chamber during the experiment. Two vials for each sample were sacrificed at the following times: 0, 1, 2, 6, 12, 24 and 48 hours. At each time interval, the centrifuge tubes were removed from the anaerobic chamber and centrifuged at 5000 rpm for 5 minutes to extract the pore water.

The pore water was then carefully pipetted out and filtered through a 0.45 µm filter. For each duplicate, the concentration of Fe^{2+} was determined by pipetting 100 µL of the filtered sample into 5 mL of Ferrozine, and the concentration determined by measuring the absorbance at 560 nm (Stookey, 1970). The remaining filtered sample was diluted using de-ionised water and stored in fridge. The dilution was done in anticipation that the samples would be analysed for SO_4^{2-} using IC in the Department of Geological Sciences at the University of Cape Town. Due to unforeseen circumstances and time constraints, the samples were sent to another laboratory for analysis by IC. Samples were placed in to the auto analyser and the corresponding sample number entered into the software. During the

University of Cape Town

process, the file containing this data was lost. For the lack of a hard copy as backup of this data, SO_4^{2-} concentrations couldn't be calculated for different samples.

Fortunately, very small volumes of the sample were left over in the vials, and it was therefore decided to use a turbidimetric method (Tabatabi, 1974) in order to analyse for SO_4^{2-}. The following reagents were prepared:

1. 0.05 M HCl
2. Stock Gelatin: Prepared by taking a slight excess over 500 mL of de-ionised water in a glass Erlenmeyer flask and heating to 70°C on a hot plate. Once a temperature of 70°C was reached, the Erlenmeyer flask was take off the heat, and 1.5 g of gelatin dissolved while using slow stirring. The solution was left to cool, and was then placed in a refrigerator overnight (a time of at least 16 hours is required).
3. Barium-Gelatin solution: The stock gelatin solution was removed from the fridge and allowed to warm slowly to room temperature. A 50 mL aliquot of this stock gelatin solution was then pipetted into an Erlenmeyer flask and 0.5 g of $BaCl_2.2H_2O$ added directly to the flask. The solution was then slowly stirred using a magnetic stirrer for 1 hour. Once this was complete, the solution was then left to stand for a further 1 hour before placing in the refrigerator overnight. This Barium-Gelatin solution is then ready for use the next day.

Standards for the method were prepared by making a 0.01 M stock solution of K_2SO_4. Dilutions of the stock solution were the made using de-ionised water to prepare standards with concentrations of 250, 500, 750, 1000, 1500, and 2000 µM.

University of Cape Town

The procedure for samples with an expected SO_4^{2-} concentration in the 0 to 3 mM range is as follows.

1. Precharge 15 mL centrifuge tubes with 5 ml of 0.05 M HCl.
2. Pipette 150 µL of sample or standard and swirl.
3. At 1 minute intervals pipette 250 µL of the barium-gelatin reagent in to the solution and swirl immediately. Do not invert the tube and do not allow the solution to touch the interior of the cap.
4. After each tube has reacted for exactly 30 minutes, swirl and measure the absorbance at 420 nm. This must be done at 1 minute intervals to maintain the 30 minute offset.

As a result of the small volumes of sample available for the analysis, 50 µL of the sample, 500 µL 0.05 M HCl, and 25 µL of the barium-gelatin reagent were used to prepare a trial run of the standards. It was found that in some instances there was not enough sample to fill the 1 mL glass micro-cuvette sufficiently to obtain a reading. The sample volume used was therefore maintained at 50 µL and the volumes of 0.05 M HCl and barium-gelatin reagent adjusted to 700 µL and 35 µL respectively. However, using these adjusted reagent volumes a calibration curve obtained in the run carried out with the samples was not adequate and the calibration curve prepared earlier was used to determine SO_4^{2-} concentrations. Although this calibration curve was prepared using slightly different reagent volumes, it was used to measure the concentrations of the samples. Thus an exact concentration for the samples was not obtained, but is considered sufficient to obtain a qualitative idea of the SO_4^{2-} concentrations. Due to time constraints the whole experiment could not be repeated.

University of Cape Town

The concentrations of Fe^{2+} and SO_4^{2-} were then plotted against time to determine the rates of iron and SO_4^{2-} reduction.

2.3.1. Fe^{2+} extractions on incubation sediments

During incubation experiments Fe^{2+} may precipitate in the sediments if there concomitant reduction of SO_4^{2-} to ΣH_2S. To extract Fe^{2+}, the top portion of the sediments in the 50 mL vials used for the incubation was discarded in case any oxidation had occurred. Approximately 1 g of sediment was then weighed out into a 15 mL VWR brand centrifuge tube to which 10 mL of 0.5 M HCl was pipetted. The vials were then placed on a shaker at a speed of 125 rpm for 1 hour. After shaking was complete, the vials were centrifuged at a speed of 5000 rpm for two and a half minutes. Without filtering, 100 µL of the supernatant was pipetted off the top and the Fe^{2+} concentration determined by using ferrozine as described above using the method of Stookey (1970).

University of Cape Town

2.4. Determination of the carbonate content of aquifer sediments

Initially the method described by Birch (1981) using the Karbonat-Bombe was going to be employed. However, the sediments were thought to contain < 10 % $CaCO_3$ and the accuracy of this method is not considered to be good for samples with a $CaCO_3$ content of < 10 %. The method described below was therefore used.

For the purposes of this study, a known mass of dry sediment (approximately 4 g) was placed into a pre-weighed beaker. Then 10 mL of a 10 % HCl solution was added to the beaker. The contents of the beaker was swirled at the start, and several times thereafter. The beakers were then left to dry in a fume hood. When completely dry, de-ionised water was then added to the beakers. This was done in order to dissolve any salts that may have formed during the drying of the samples. If present these salts would contribute to the weight of the dried sample thus giving erroneous results. The samples were then placed back into the fume hood to dry again. The final weight of the beakers was measured only once the samples were completely dry. A scale accurate to three decimal places was used to weigh the samples. The carbonate content of the samples was then calculated as follows:

$$\text{Carbonate content (weight \%)} = \left\{\frac{\text{Initial weight - Final weight}}{\text{Initial weight}}\right\} \text{x } 100$$

University of Cape Town

2.5. Porosity

Syringes were weighed prior to, and after insertion of wet sediment into the syringes and the mass was determined by difference. The volume of sediment was also recorded. The sediment was then placed into pre-weighed beakers, and the syringes rinsed with water in order to ensure that all the sediment had been removed. These were then placed in an oven to allow the water to evaporate. After the sediment had completely dried, the beakers were weighed again and the mass of the dry sediment calculated by difference.

The porosity of all sediment samples was calculated using the proxy of water, and assuming a density of water to be 1 $g.cm^{-3}$, as follows:

$$\phi = \left\{\frac{\text{Wet Mass (g) - Dry Mass (g)}}{\text{Volume (cm}^3\text{)}}\right\} 100$$

2.6. Grain size analysis

The grain size distribution of five sediment samples was determined as follows. The sediment samples were placed on wax paper and air dried prior to commencing the analysis. Once dry, the samples were split into smaller portions using the method of coning until approximately 15 to 20 g of the original bulk sample remained. Dry sieving was then used to separate the sample into < 2 mm fraction and > 2 mm (gravel) fractions and the gravel fractions weighed. The sand (> 0.063 mm) and mud fractions (< 0.063 mm) were then separated using wet sieving. The two different size fractions were then placed into an oven to dry, and the weighed. As previously mentioned the Cape Flats aquifer sands contain very little clay. As a result thereof, it was decided not to separate the mud size fraction into the silt and clay fractions, as this would require sieving of large quantities of the sediment in order to obtain enough of the mud size fraction to perform a separation into clay and silt fractions.

University of Cape Town

CHAPTER 3 - RESULTS

1. GROUNDWATER ANALYSES

The results of all analyses carried out on groundwater samples have been tabulated in appendix B. A comparison of all the mean cation and anion concentrations (as well as the ranges) within and outside the plume, as well as field measurements taken are tabulated in Table 3.1. The purpose for doing this is to make the comparison of background values with those inside the plume easier. When referring to samples inside the plume, the author is referring to all samples except GM35 and background samples (GM48, GM49, GM50).

The pH of the groundwater from background boreholes is neutral (7.0 to 7.2) while the pH of groundwater from within the contaminant plume is slightly acidic to neutral and ranges fro 6.1 to 7.1. The lowest pH measurement of 6.1 was made closest to the product spillage position at GM 4. The Eh is negative in all of the groundwater samples within the contaminant plume and values range from -13 mV at GM37 to -221 mV at GM31. Values ranged between 42 and 62 mV in background samples. Alkalinities in background samples ranges between 8.5 and 9.5 mM. The alkalinities of the samples measured within the plume are variable and range from 4.1 mM to 10.1 mM. The highest alkalinities were recorded closest to where the spillage occurred. The measured EC is highest in background water samples (up to 1533 µS/cm) while samples from the contaminant plume were generally lower except at GM 27. The lowest measured EC within the plume is 391 µS/cm.

The reduced inorganic species concentrations of Fe^{2+}, NH_4^+, and ΣH_2S are highest in contaminated groundwater samples. However, the mean value for Mn^{2+} suggests that higher concentrations were found in background water samples. SO_4^{2-} and NO_3^- are highest in background water samples and lowest in groundwater samples from within the contaminant plume. However, concentrations similar to the background concentrations were measured for NO_3^- (1164 μM) and SO_4^{2-} (1242 μM) within the plume at GM37 and GM27 respectively.

Table 3.1. Mean inorganic analyses in contaminated and uncontaminated groundwater.

Parameter	Background samples [a]		Contaminated samples [b]	
	Average	**Range**	**Average**	**Range**
pH	**7.1**	7.0 – 7.2	**6.7**	6.1 – 7.1
EC (μS/cm)	**1499**	1466 – 1533	**1044**	391 – 1436
Eh (mV)	**52**	42 – 62	**-101**	-13 - -221
Alkalinity (mM) [c]	**9.1**	8.5 – 9.5	**8.0**	4.1 – 10.1
Fe^{2+} (μM)	**0**	0	**355**	14 – 978
Mn^{2+} (μM)	**2.4**	1.4 – 4.7	**1.8**	0.4 – 8.4
NH_4^+ (μM)	**4**	3 – 5	**221**	75 – 432
NO_3^- (μM)	**998**	645 – 1185	**125**	0 – 1164
SO_4^{2-} (μM)	**1184**	1072 – 1119	**209**	0 – 1242
ΣH_2S (μM)	**0.8**	0.7 – 1.0	**7.5**	1.8 – 25.3

[a] Mean values for inorganic parameters from uncontaminated water based on 3 sampling sites (GM 48, GM 49, and GM 50). GM 35 was excluded.

[b] Mean values of inorganic parameters from contaminated water based on all other sampling sites (n=28)

[c] Total alkalinity

University of Cape Town

1.1. Spatial variation of groundwater chemistry

In order to assess the processes occurring at the site, contour plots of the measured concentrations of ΣH_2S, SO_4^{2-}, Fe^{2+}, NO_3^-, NH_4^+, Mn^{2+}, and total alkalinity were generated in Surfer® version 6.04 using Kriging. These are shown in Figures 3.1 (a) – (g) respectively. Due to the fact that the boreholes at the site were only a few metres deep, it must be noted that the contour plots generated can only be used to asses the spatial distribution in 2-D space. Vertical profiling of the inorganic species could not be carried out as the depth of the boreholes did not allow this.

University of Cape Town

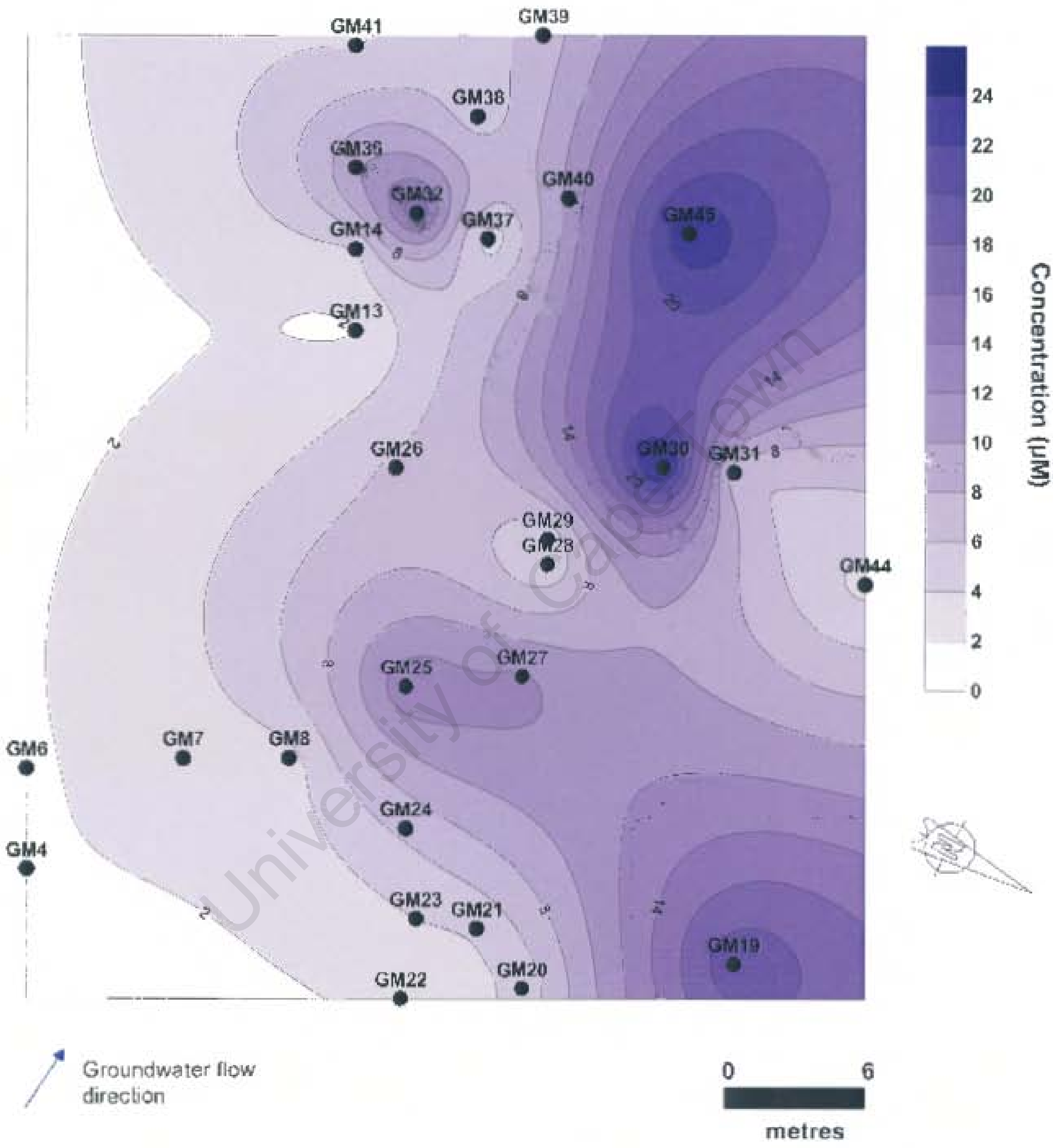

Figure 3.1a. Contour Plot showing the distribution of groundwater ΣH_2S concentrations across the site.

University of Cape Town

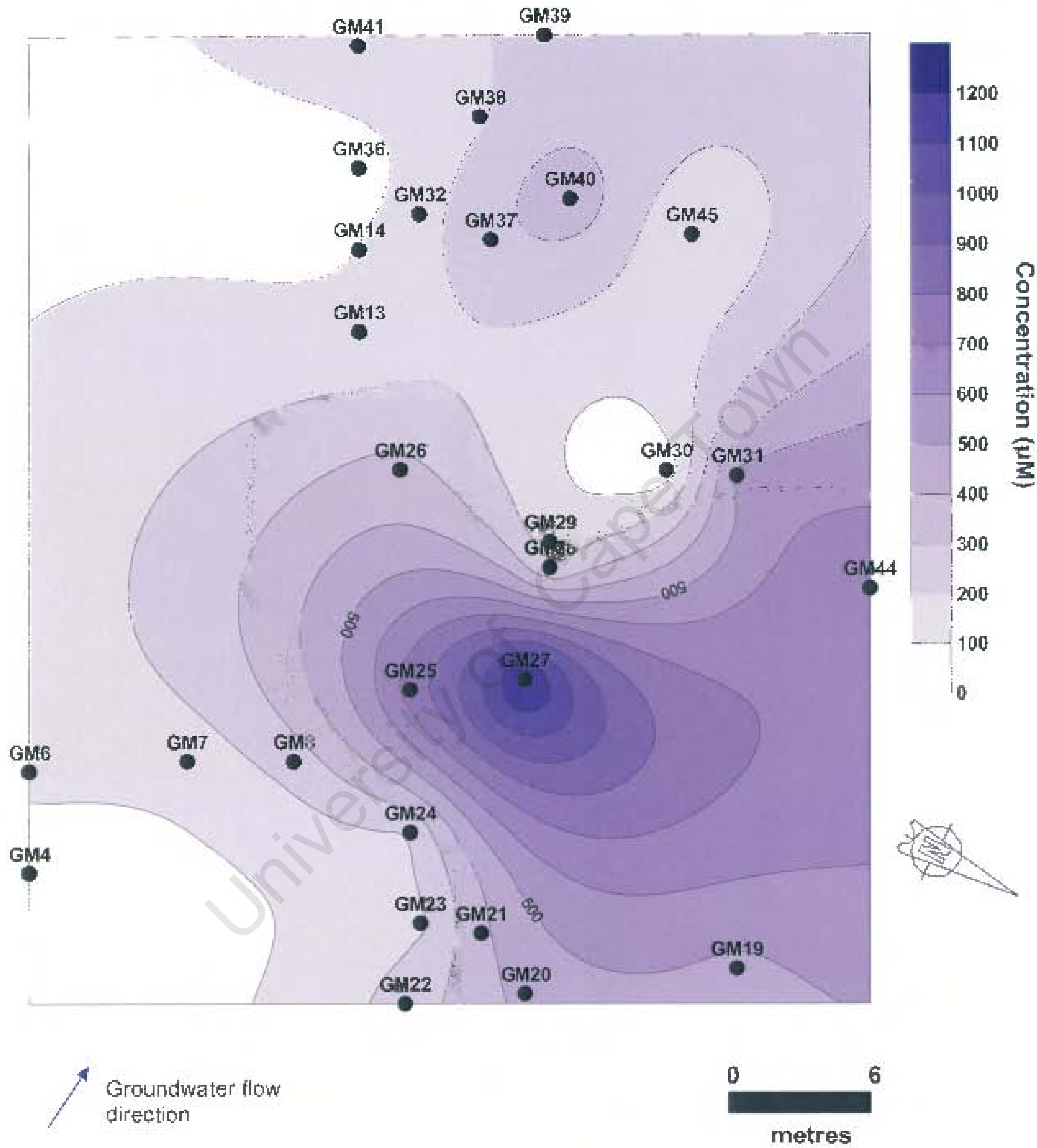

Figure 3.1b. Contour Plot showing the distribution of groundwater SO_4^{2-} concentrations across the site.

University of Cape Town

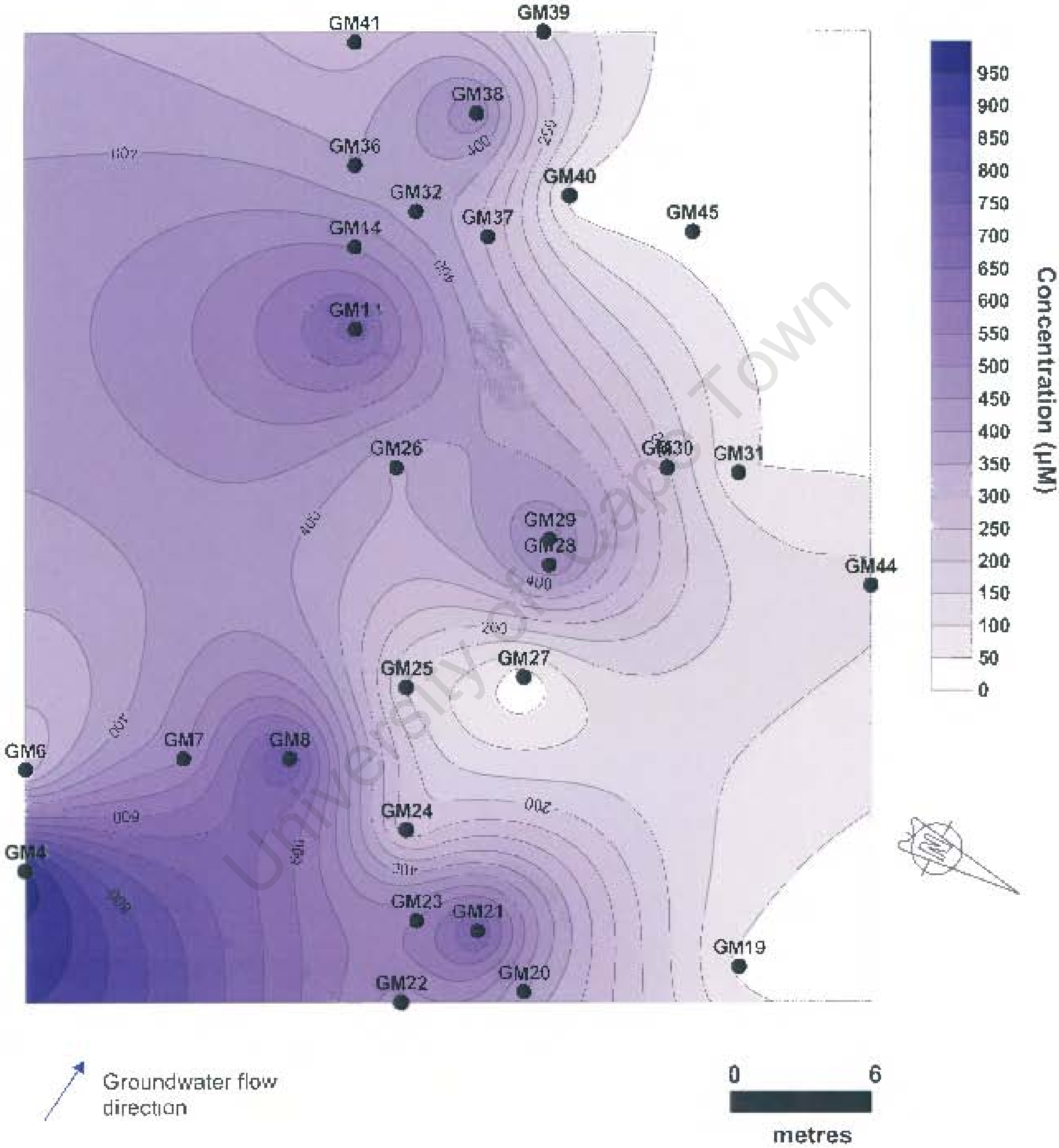

Figure 3.1c. Contour Plot showing the distribution of groundwater Fe^{2+} concentrations across the site.

University of Cape Town

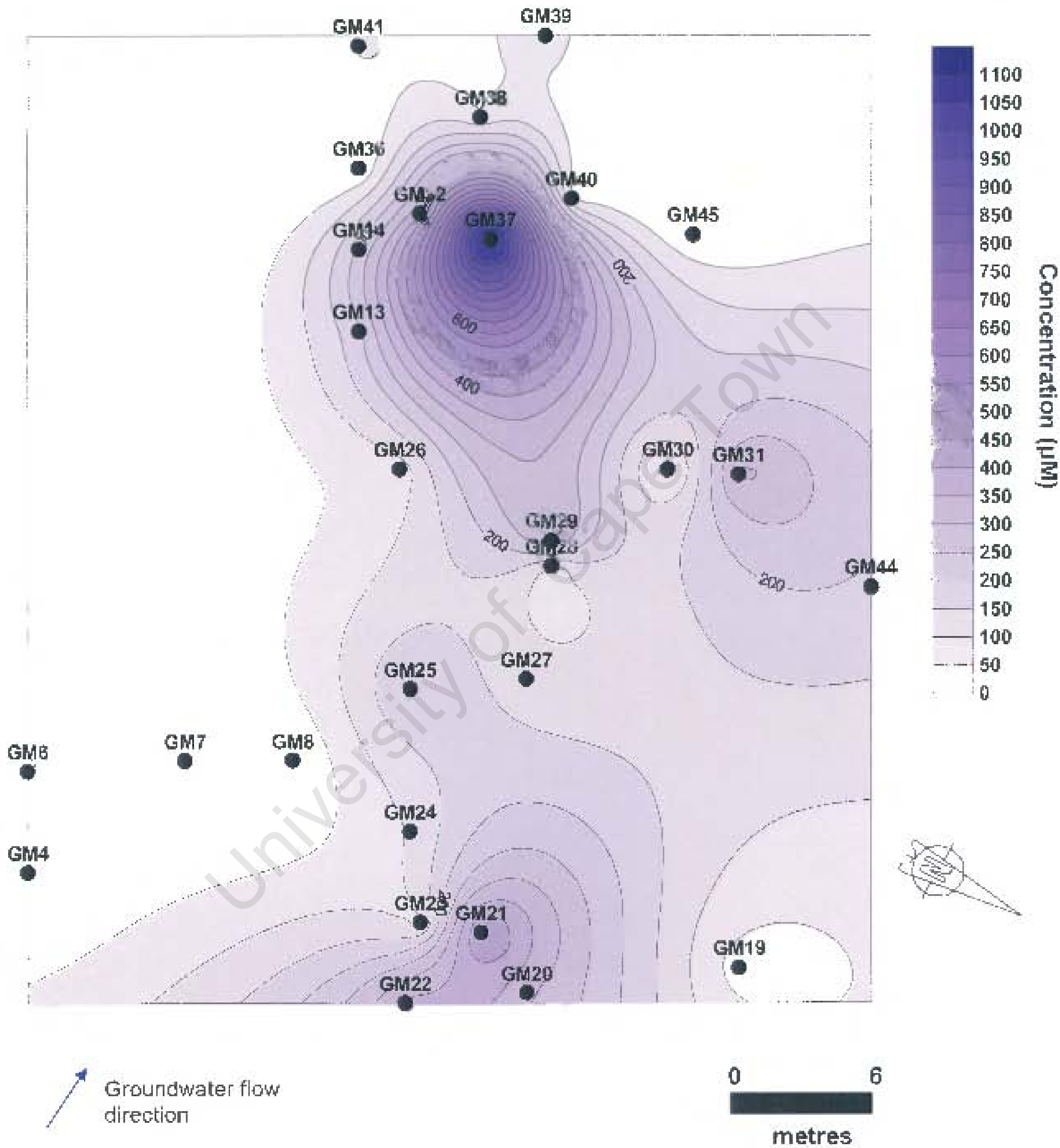

Figure 3.1d. Contour Plot showing the distribution of groundwater NO_3^- concentrations across the site.

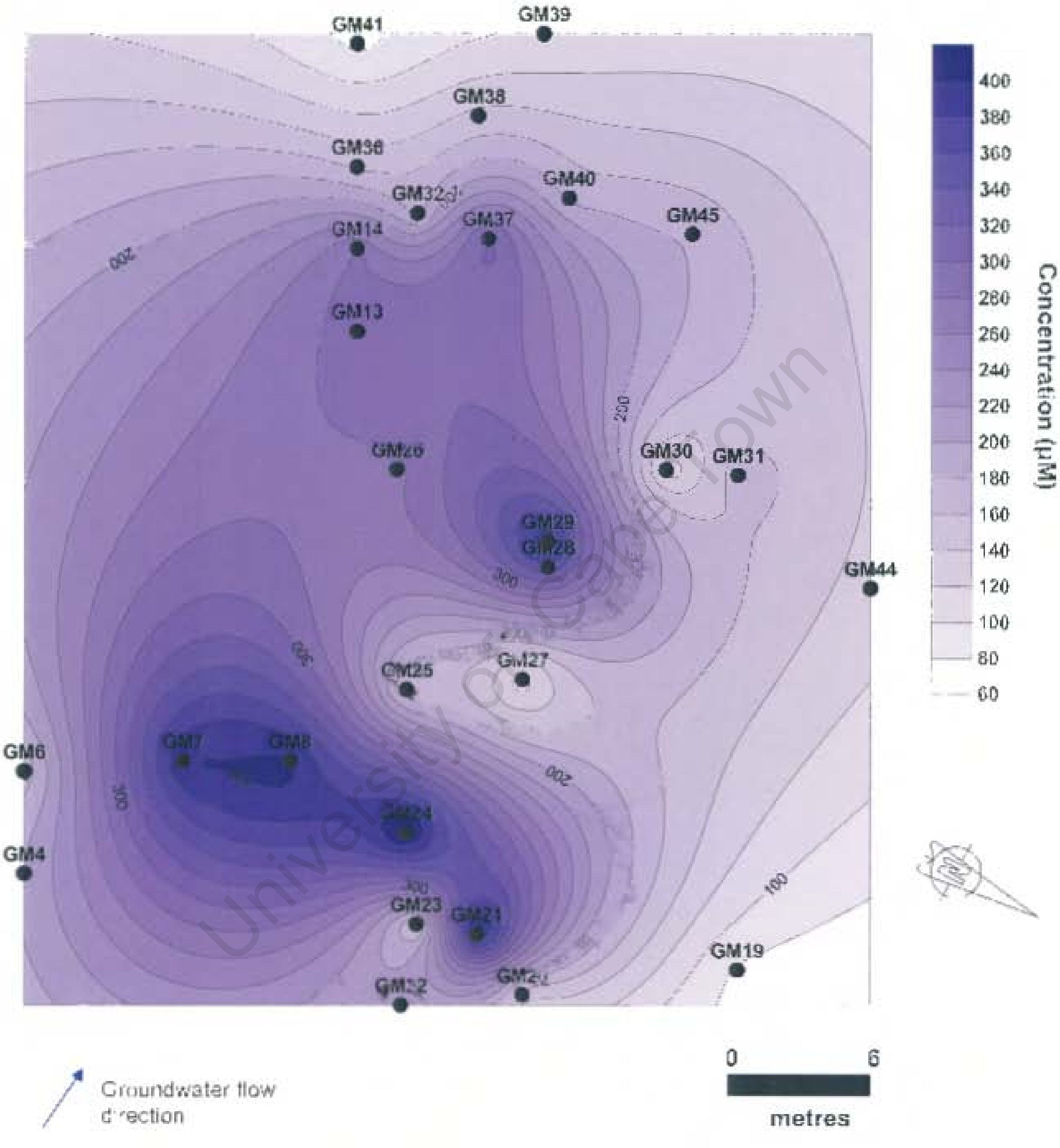

Figure 3.1e. Contour Plot showing the distribution of groundwater NH_4^+ concentrations across the site.

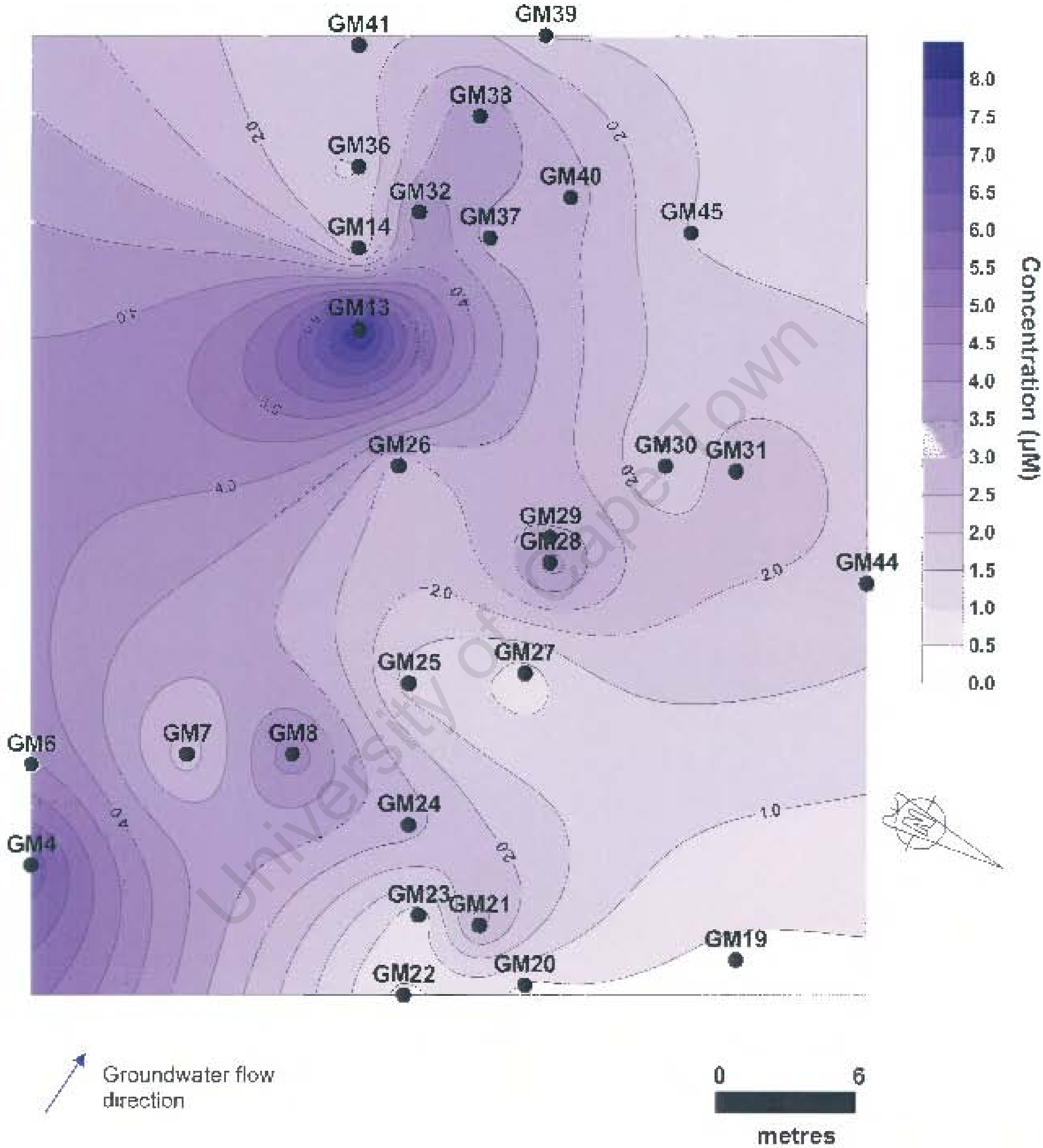

Figure 3.1f. Contour Plot showing the distribution of groundwater Mn^{2+} concentrations across the site.

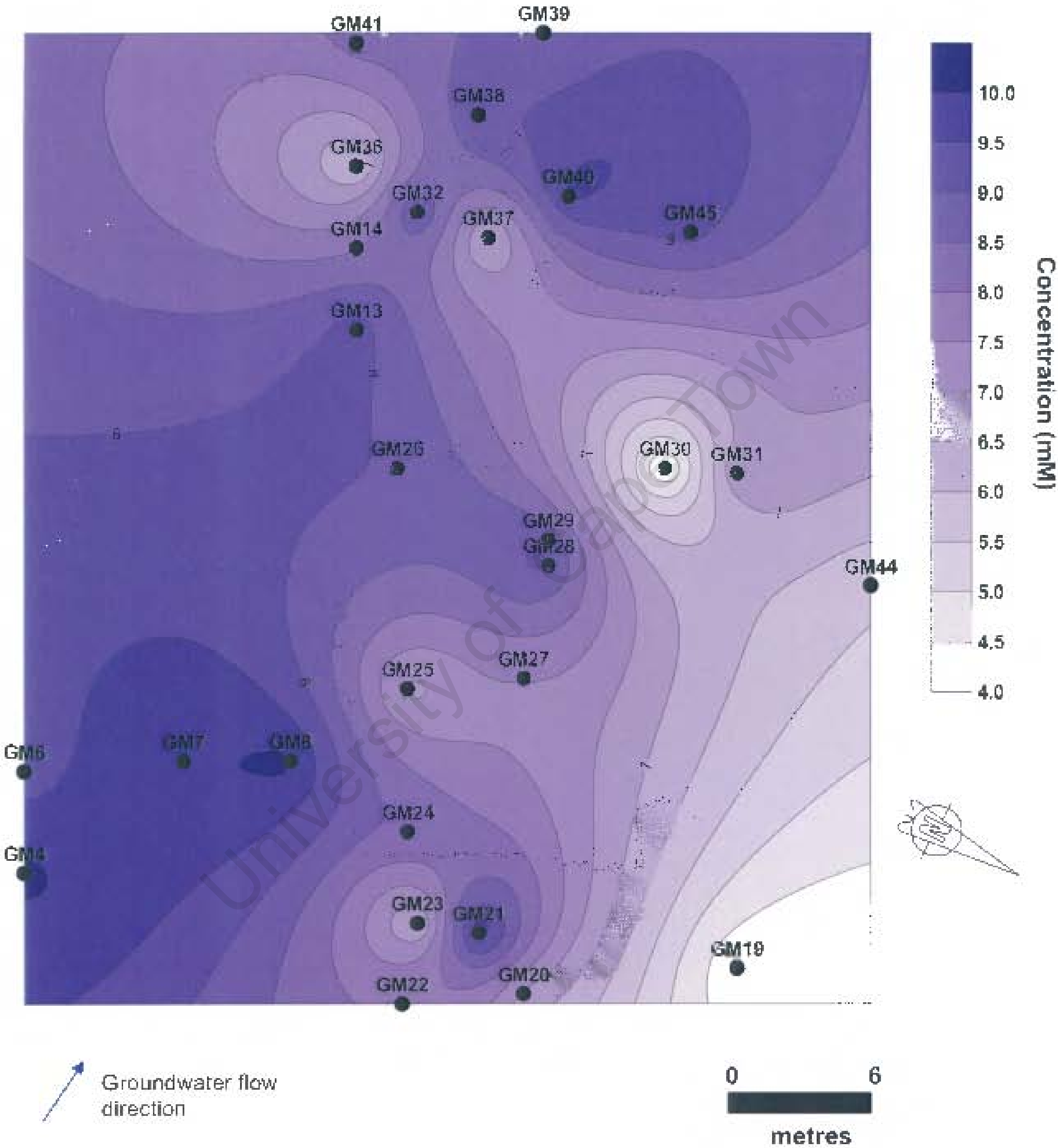

Figure 3.1g. Contour Plot showing the measured groundwater alkalinities across the site.

University of Cape Town

2. SEDIMENT PROPERTIES

2.1. Iron oxide extractions

Two sets of extractions were carried out on sediment samples taken from the site. The results of these sediment extractions are discussed below.

2.1.1. Set 1 – Extractable iron from samples taken above and below the water table

The first set of extractions was performed to deduce how the concentrations of extractable iron oxyhydroxides (extracted using an ascorbate solution) and reactive iron oxides (using a buffered sodium dithionite solution) varied between samples taken at a depth of 40 cm below the surface, and samples taken at the depth of the water table. The extracts were then analysed for total iron using ferrozine reductant as described in Chapter 2. Results are shown in Figure 3.2.

From Figure 3.2 it is observed that the amount of iron extracted using buffered sodium dithionite is similar in samples B and E for samples taken from near the surface and close to the water table. Samples A and 26 display some differences in the extracted concentrations. The most noticeable is in sediment sample A in which the iron concentrations are highest in the sample taken near the surface. In contrast to this, the iron extracted from the sample 26 is higher in the sample taken at the level of the water table is higher than the sample taken near the surface.

Iron concentrations extracted using the ascorbate solution were higher in all samples taken near the water table except in samples B, E, and 26 but not in sample A.

University of Cape Town

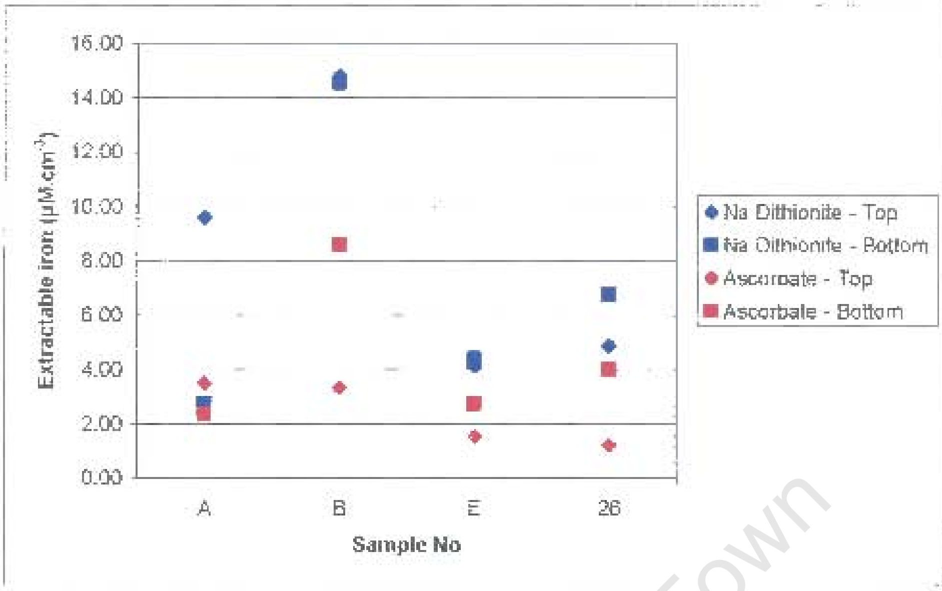

Figure 3.2. Total iron concentrations extracted from sediment samples taken at different depths using solution of buffered sodium dithionite and ascorbate solution. 'Top' refers to samples taken 40 cm below surface and 'Bottom' refers to samples taken at the depth of the water table.

University of Cape Town

Both the ascorbate and sodium dithionite leachates from this set of sediment extractions were analyses for Mn using (atomic absorption spectrometry) AAS. The results are shown in Table 3.2 and indicate that very little Mn is extracted from sediments.

2.1.2. Set 2 – Extractable Fe^{3+} and Fe^{2+} on samples taken below the groundwater table

The second extraction was only performed on samples taken from the depth of the water table. Once the extractions were complete the ascorbate and sodium dithionite leachates samples were analysed for Fe^{2+} and total Fe using the method of Stookey (1970) as described in Chapter 2. Results of the extraction are shown in Figure 3.3.

Table 3.2. Extractable Mn from sediments taken above and below the water table using ascorbate and sodium dithionite solutions. All concentrations expressed as μM.cm^{-3}.

	Sample No	Ascorbate	Sodium dithionite
Top	A	0.04	0.0003
	B	< 0.008	0.0003
	26	< 0.008	0.0003
	D	< 0.008	0.0005
	E	< 0.008	0.0004
Bottom	A	< 0.007	0.0003
	B	< 0.008	0.0003
	26	< 0.008	0.0003
	D	< 0.008	0.0003
	E	0.128	0.0003

University of Cape Town

Figure 3.3. shows that Fe^{2+} and total Fe concentrations in the buffered sodium dithionite are almost identical in samples A, E, 13, 26, and 27, while total iron concentrations were higher in sample B. Fe^{2+} and total iron concentrations in the ascorbate extracts are very similar for samples 13 and 26 while the others displayed minor differences with Fe^{2+} being slightly lower in sample E, but higher in samples A, B, and 27.

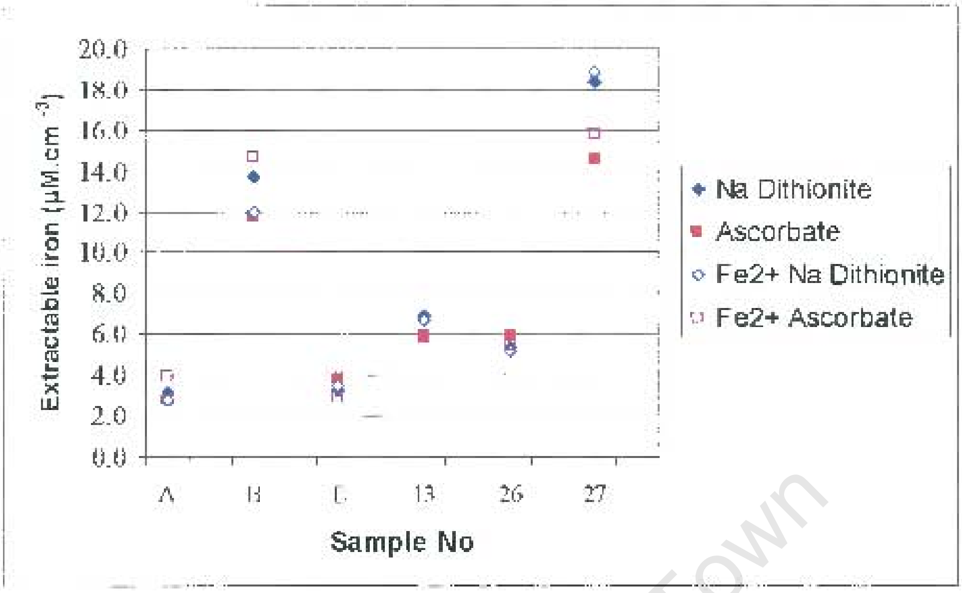

Figure 3.3. Plot showing the total iron and Fe^{2+} concentrations extracted from samples taken at the depth of the water table. Results shown are an average of duplicates.

University of Cape Town

2.2. Sediment incubations

2.2.1. Pore water Fe^{2+} and SO_4^{2-}

The measured pore water Fe^{2+} concentrations measured over the period in which the incubation was performed fluctuated quite considerably over the first 12 hours in both samples (Figure 3.4 and 3.5). After the first 12 hours the concentrations then appear to increase at a more consistent rate. The overall trend shows that Fe^{2+} concentrations increased over the duration of the incubation in both samples 26 and 27. It should also be noted that the Fe^{2+} concentration at t=0 (7 µM) in sample GM26 is very different to that which was measured in the groundwater (346 µM). This difference was not as great in sample GM27 where the measured concentration at t=0 is 0 µM compared to a concentration of 14 µM that was measured in the groundwater.

SO_4^{2-} concentrations decreased rapidly in the first hour of the incubation in samples 26 and 27 (Figures 3.6 and 3.7). After the first hour had elapsed the SO_4^{2-} concentrations generally remained fairly constant. In sample 26 the SO_4^{2-} concentration increased from 34 µM after 6 hours to 120 µM after 12 hours, and decreased to 37 µM after 24 hours had elapsed. The concentration of SO_4^{2-} at t=0 in sample GM26 (300 µM) was very similar to that measured in the groundwater (333 µM). As previously noted, GM27 seems to have anomalously high SO_4^{2-} concentrations in the groundwater (1242 µM) compared to other samples, and a SO_4^{2-} concentration of 583 µM was measured at t=0.

2.2.2. Fe^{2+} extraction on incubation sediments

Fe^{2+} extracted from the incubation sediments fluctuates over time in both samples 26 and 27 (Figures 3.8 and 3.9). However, the general trend over time in sample GM27 is that the extractable Fe^{2+} from the sediments increases over time. This increase was not observed in sample GM26.

University of Cape Town

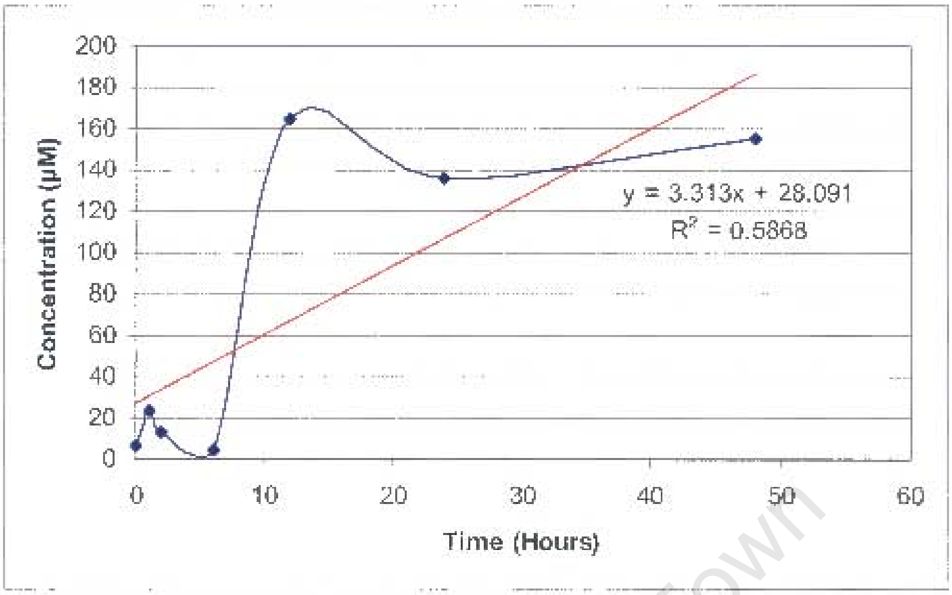

Figure 3.4. Pore water Fe^{2+} concentrations over a 48-hour incubation period for sediment sample 26.

University of Cape Town

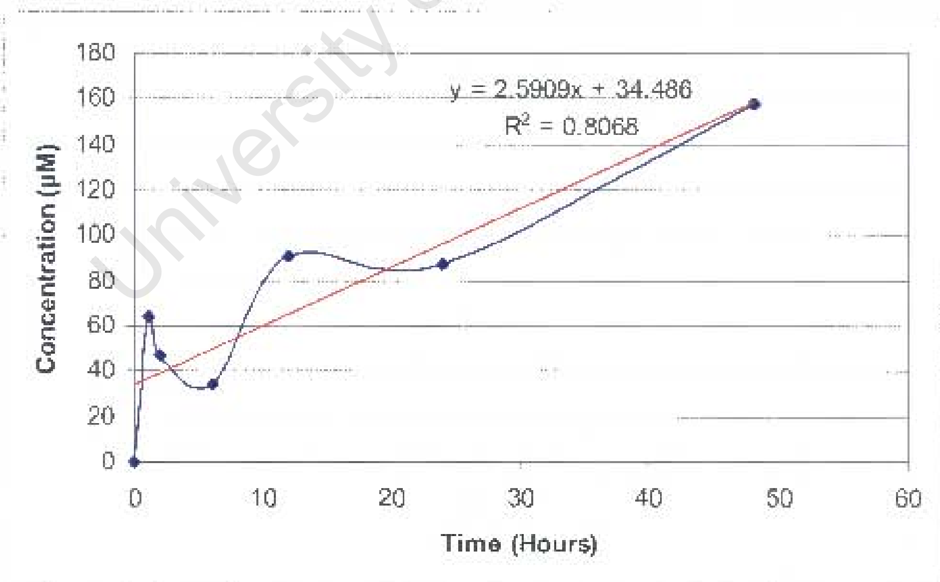

Figure 3.5. Pore water Fe^{2+} concentrations over a 48-hour incubation period for sediment sample 27.

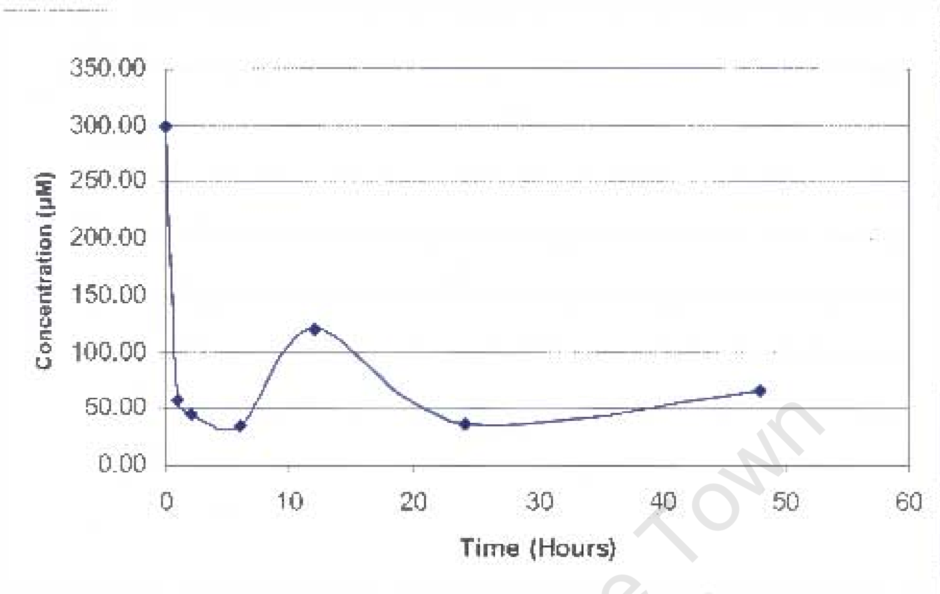

Figure 3.6. Pore water SO_4^{2-} concentrations over a 48-hour incubation period for sediment sample 26.

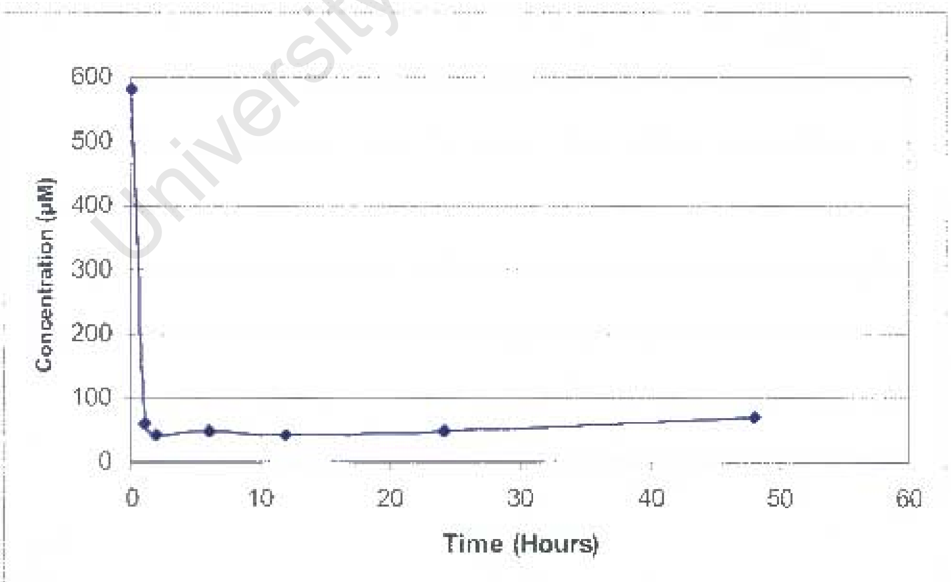

Figure 3.7. Pore water SO_4^{2-} concentrations over a 48-hour incubation period for sediment sample 27.

University of Cape Town

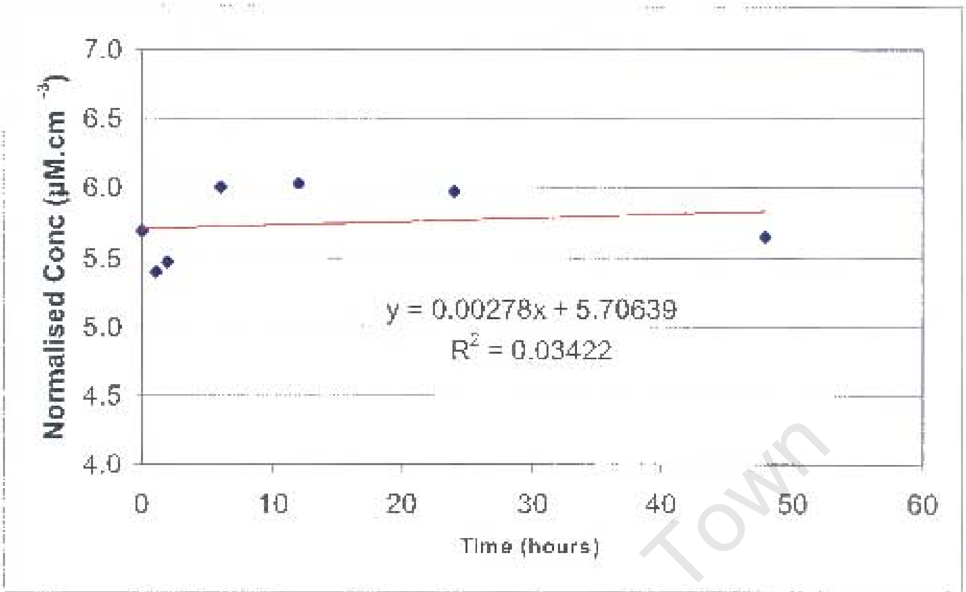

Figure 3.8. Fe^{3+} reduction rates measured as the accumulation of extractable Fe^{2+} in sediment sample GM26 using 0.5 M HCl.

University of Cape Town

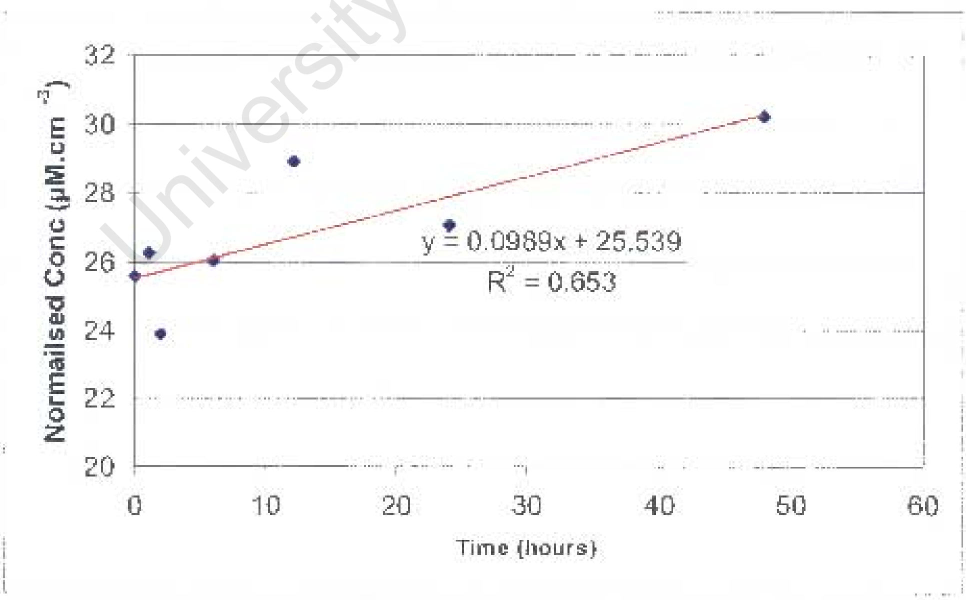

Figure 3.9. Fe^{3+} reduction rates measured as the accumulation of extractable Fe^{2+} in sediment sample GM27 using 0.5 M HCl.

2.3. Porosity

The results obtained from the porosity determinations reveal that the porosity of all of the samples is essentially consistent throughout the site (Table 3.3).

Table 3.3. Results of sediment porosity determinations

	Sediment sample number					
	A	**B**	**E**	**13**	**26**	**27**
Volume (cm^3)	9.6	9.8	7.0	7.2	6.8	8.2
Wet mass (g)	18.75	20.40	15.21	16.00	14.21	17.46
Dry mass (g)	15.38	16.96	12.71	13.47	11.92	14.56
Porosity (%)	35	35	36	35	34	35

University of Cape Town

2.4. Grain size analysis

Results of the grain size analysis performed on five sediment samples using wet and dry sieving are tabulated in Table 3.4. All of the sediments sampled are comprised of ≥ 95 % sand, and minor amounts of gravel and mud.

Table 3.4. Results of grain size analysis determinations expressed as a percentage of the bulk sample.

	SED A	**SED B**	**SED C**	**SED D**	**SED E**
Gravel	3	4	3	0	0
Sand	96	95	96	100	100
Mud	0	1	1	0	0

2.5. Carbonate determination

The concentrations of carbonates in the sediments is low (< 0.2 weight %) in samples taken from above and below the groundwater.

Table 3.5. Carbonate contents of sampled sediments

Sample number	Carbonate content (weight %)
A TOP	0.1
A BOTTOM	0.0
B TOP	0.0
B BOTTOM	0.0
E TOP	0.1
E BOTTOM	0.0
13 TOP	0.1
13 BOTTOM	0.0
26 TOP	0.2
26 BOTOM	0.1
27 TOP	0.0
27 BOTTOM	0.1

University of Cape Town

3. ANALYTICAL APPRAISAL

The EN was calculated for all samples in order to determine if there is a reasonable charge balance of cations and anions from the analyses received (Appendix C). It is concluded that generally the analysis of the samples is 'good' as the EN is less than 5 % for most samples. The EN was less than 10 % in all samples except GM35 which had an EN of 24 % indicating an excess of cations, or that an anion which is present has either not been analysed for or detected by the analytical method that was used.

CHAPTER 4 - DISCUSSION

1. PROCESSES OCCURRING AT THE SITE

1.1. Nitrate reduction

The depletion of NO_3^- and the production of NH_4^+ indicate that dissimilatory nitrate reduction is occurring at the site. The lowest measured levels of NO_3^- occur closest to the point where the spillage occurred (Figure 3.1d). This is due to the fact that NO_3^- reduction has been occurring the longest closest to this point. Based on historical data, the highest BTEX concentrations were found closest to the point where the spillage occurred at GM9 (no BTEX analyses were carried out on samples taken closer to the spillage position). Based on the stoichiometry of the hydrocarbon degradation reaction using NO_3^- as a TEA, more NO_3^- will be consumed by the reaction where hydrocarbon concentrations are highest. This is consistent with what is observed at the site. The concentration of NO_3^- in GM36 is also low and is located downgradient in the direction of groundwater flow from GM4, GM6, GM7, and GM8. This may be as a result of NO_3^- depleted groundwater moving in this direction. However due to the lack of sampling wells in this area this cannot be confirmed. Higher levels of NO_3^- occur in GM20, GM21, GM22, and GM23 which may be explained by recharge of NO_3^- rich groundwater entering the study area. The high concentrations of NO_3^- in GM37 are similar to those found in background samples, the reasons for which are still unknown at this stage.

University of Cape Town

The highest concentrations of NH_4^+ were also found closest to the point where the spillage occurred in GM7, GM8, and GM24 (Figure 3.1e). In Figure 3.1e it is also noted that the highest NH_4^+ concentration are found within the centre of the plume, and decreases towards the plume edge. Cozzarelli *et al.* (1999) found that significant concentrations of N_2O were found in only in the shallowest samples which are most affected by the infiltration of oxygen and nitrate enriched groundwater. These results were consistent with other studies which found that the denitrification reaction would be favoured in a more oxidised environment where the low carbon to electron ratios occurred. It is thought that denitrification may be occurring in groundwater samples taken at the edges of the plume. This may possibly account for the lower NH_4^+ concentrations found in samples GM4, GM6, GM19, GM20, GM22, GM39, GM41, and GM44. At these sampling positions, conditions may be more oxidising where anaerobic groundwater meets more oxygenated groundwater. If this is the case, then lower carbon to electron acceptor ratios may occur. A lower ratio may arise from the degradation of the hydrocarbons occurring under more oxygenated conditions thereby reducing the dissolved oxygen and hydrocarbon concentrations. The lower hydrocarbon concentration would therefore result in a lower carbon to electron acceptor ratio as the TEA (NO_3^-) concentration remains the same but the hydrocarbon concentration has been reduced. Evidence for denitrification does not exist as nitrogen and BTEX concentrations were not analysed for.

Although the importance of denitrification at the site is unknown, where large amounts of organic carbon are present, such as at this site, it is thermodynamically favourable for NO_3^- reduction to occur forming NH_4^+ (Bulger *et al.*, 1990). Dissimilatory reduction rather than denitrification is therefore considered to be the major process taking place that is responsible for removing NO_3^- from the groundwater. The depletion of NO_3^- at GM19, GM28, and GM30, along with the low concentrations of NH_4^+, indicates that nitrate reduction occurs on a small scale or in microenvironments at the site. Nitrate reduction was also

University of Cape Town

found to occur in microenvironments in a study carried out by Cozzarelli *et al.* (1999) on a gasoline contaminated aquifer.

There is great concern regarding the vulnerability of the aquifer to pollution as nitrate levels substantially exceed the maximum allowable limit (drinking water quality criteria) of 161 µM in places. These high nitrate levels are a result of the numerous agricultural activities in the area (Meyer 2000). Background nitrate levels in samples GM48, GM49 and GM50 are up to almost eight and a half times higher than the maximum allowable limit for drinking water quality. Recharge of nitrate rich groundwater at the site may therefore be playing a significant role in the intrinsic bioremediation at the site.

University of Cape Town

1.2. Manganese reduction

Manganese analysed by AAS occurs mainly as Mn^{2+} at the measured pH's at the site. The concentrations of Mn^{2+} in the background samples GM48, GM49, and GM50 is highly variable with concentrations varying from 0.4 µM to 4.7 µM in GM48 and GM50 respectively. Mn^{2+} concentrations are also variable within contaminated samples which probably reflects small scale heterogeneities at the site. The highest concentrations of Mn^{2+} were found closest to the spillage position in GM4, GM6, and GM8 (Figure 3.1f). The highest concentration is found at GM13 and is located downgradient from the product spillage position in the direction of groundwater flow. This may be indicative of groundwater in which manganese reduction was occurring close to the spillage position that has migrated to the downgradient position at GM13.

Reduction of Mn^{4+} to Mn^{2+} is occurring at the site but is not considered to be an important process contributing to intrinsic bioremediation due to the low concentrations of extractable Mn as determined from sediment extraction results (Table 3.2).

1.3. Iron and sulphate reduction

The elevated concentrations of Fe^{2+} and ΣH_2S in certain areas of the site are indicative that the reduction of both Fe^{3+} and SO_4^{2-} is occurring at the site. The high concentrations of Fe^{2+} are found closest to the point where the spillage occurred in boreholes GM4, GM7, and GM8 (Figure 3.1c), and downgradient from the point where the spillage occurred. High concentrations that are found downgradient may result from the migration of high iron groundwater migrating along the groundwater flow path. These high Fe^{2+} concentrations in these boreholes, along with the low ΣH_2S concentrations (Figure 3.1a) suggest that Fe^{3+} reduction, rather than SO_4^{2-} reduction, is the predominant process taking place.

Chapelle and Lovley (1992), in a study carried out on the Middendorf aquifer in South Carolina, showed that high concentrations of dissolved iron in groundwater develop only if there is little or no sulphate reduction occurring. Results showed that the activity and interaction of Fe^{3+} and SO_4^{2-} reducing microorganisms in the aquifer are responsible for the development and localisation of high iron groundwater. Fe^{3+} reducers are thought to contribute to the development of the high iron zone by inhibiting the activity of sulphate reducing microorganisms. Both Fe^{3+} and SO_4^{2-} reducers compete for certain substrates such as hydrogen and organic substrates. In high iron zones, Fe^{3+} reducers are able to maintain the levels of these substrates below levels that are required for significant activity of sulphate reducers. The production of Fe^{2+} exceeds the production of ΣH_2S and Fe^{2+} accumulates in solution.

University of Cape Town

Other mechanisms for the reduction of Fe^{3+} have also been proposed. Fe^{3+} has been reported to be reduced by sulphide via the following reaction (Appelo & Postma, 1994):

$$2FeOOH + 3HS^{-} \rightarrow 2FeS + S^{0} + H_2O + 3OH^{-}$$

In this reaction part of the sulphide reduces Fe^{3+} and produces S^0, while the remainder of the dissolved sulphide precipitates as FeS. In a study by Coleman *et al.* (1993) on siderite concretions in salt marsh sediments, it has been proposed that instead of reducing Fe^{3+} indirectly through the production of sulphide, some bacteria can reduce Fe^{3+} directly through an enzymatic mechanism. This mechanism produces siderite rather than iron sulphides.

Figure 3.1b shows that SO_4^{2-} has been removed from the groundwater near to the point where the spillage occurred. However, from Figure 3.1a it is also noted that low ΣH_2S concentrations are found in this area. The precipitation of ΣH_2S with Fe^{2+} to form FeS is the most likely process taking place that would account for the removal of sulphide. If the precipitation of FeS is taking place, then this serves as evidence that the reduction of Fe^{3+} and SO_4^{2-} are occurring concomitantly at the site. The high concentration of Fe^{2+} in the water suggests that the production of Fe^{2+} exceeds the production of ΣH_2S.

These two processes are considered to be of great importance at the site. The proximity of the site to the coast means that aquifer is recharged with both SO_4^{2-} rich meteoric water percolating downwards through the sands, and SO_4^{2-} rich groundwater.

University of Cape Town

1.4. Methanogenesis

Initially, prior to commencing sampling, it was thought to be unlikely that methanogenesis is occurring at the site. Reduction of Mn^{4+} does not seem to be significant at the site but reduction of NO_3^-, SO_4^{2-}, and Fe^{3+} are taking place. The theoretical redox sequence may therefore be approaching the end and thus methanogenesis may become significant at the site. From the theoretical redox sequence it is expected that methane containing groundwaters are usually low in sulphate. SO_4^{2-} concentrations within the plume are significantly lower than in background samples and no SO_4^{2-} was detected in GM 4. The possibility that the formation of CH_4 may be occurring at the site therefore cannot be ruled out. Further studies are required in order to ascertain the importance of methanogenesis at the site.

There are two predominant processes that may be occurring for the formation of methane (Appelo & Postma, 1994). The first is the reduction of CO_2 via the following reaction:

$$CO_2 + 4H_2 \rightarrow 2H_2O + CH_4$$

The second reaction that may contribute to the formation of CH_4 is the fermentation of organic matter, for example, acetate:

$$CH_3COOH \rightarrow CH_4 + CO_2$$

University of Cape Town

1.5. Spatial delineation of redox processes based on criteria of Lyngkilde and Christensen (1992)

In several studies carried out (Champ *et al.*, 1979; Lyngkilde & Christensen, 1992; Bjerg *et al.*, 1995; Postma & Jackobsen, 1996; Norkus *et al.*, 1996; Ludvigsen *et al.*, 1998) it has been possible to identify a distinct sequence of redox zones. These redox zones sequences are often consistent with thermodynamical principles. To distinguish these zones at the site currently under investigation has been difficult. This can be related to the speed of the groundwater flow at the site. The topography of the Cape Flats, as suggested by the name, is flat and the flow of groundwater is thus relatively slow. When groundwater flow is fast, a zonation reflecting typical redox zonation is observed, and if slow then an overlapping of these zones tends to occur. The situation at the site is the latter and accounts for the overlapping of the redox zones that is observed.

The criterion of Lyngkilde and Christensen (1992) for assigning redox status to groundwater samples (see Table 1.4) was applied to the results attained in this study. By applying these criteria to this site, it is found that methanogenesis may well be occurring in samples that were taken close to where the spillage occurred (GM4, GM7, and GM8). This makes sense as anaerobic degradation of the hydrocarbons has been taking place the longest in the area close to the spillage and thus other electron acceptors would be the most depleted at this point. Methanogenesis may also be occurring at GM36 and GM45. In a study carried out on a shallow sandy aquifer in Rømø, Denmark, Jakobsen and Postma (1999) found that Fe^{3+} reduction, sulphate reduction, and methanogenesis occur concomitantly at some sites. These cases of concomitant redox processes were investigated and it was found that there appears to be a relation between the rate of iron oxide and sulphate reduction and the occurrence of methanogenesis. When iron oxide and SO_4^{2-} reduction rates are high,

University of Cape Town

methanogenesis occurred below the iron and SO_4^{2-} reducing zone. This indicates that the conditions for methanogenesis are unfavourable. When these are low, methanogenesis overlaps concomitant iron oxide and SO_4^{2-} reduction.

Figure 4.1 shows the area in the site where NO_3^-, Fe^{3+}, SO_4^{2-}, and methanogenesis are interpreted to be occurring.

University of Cape Town

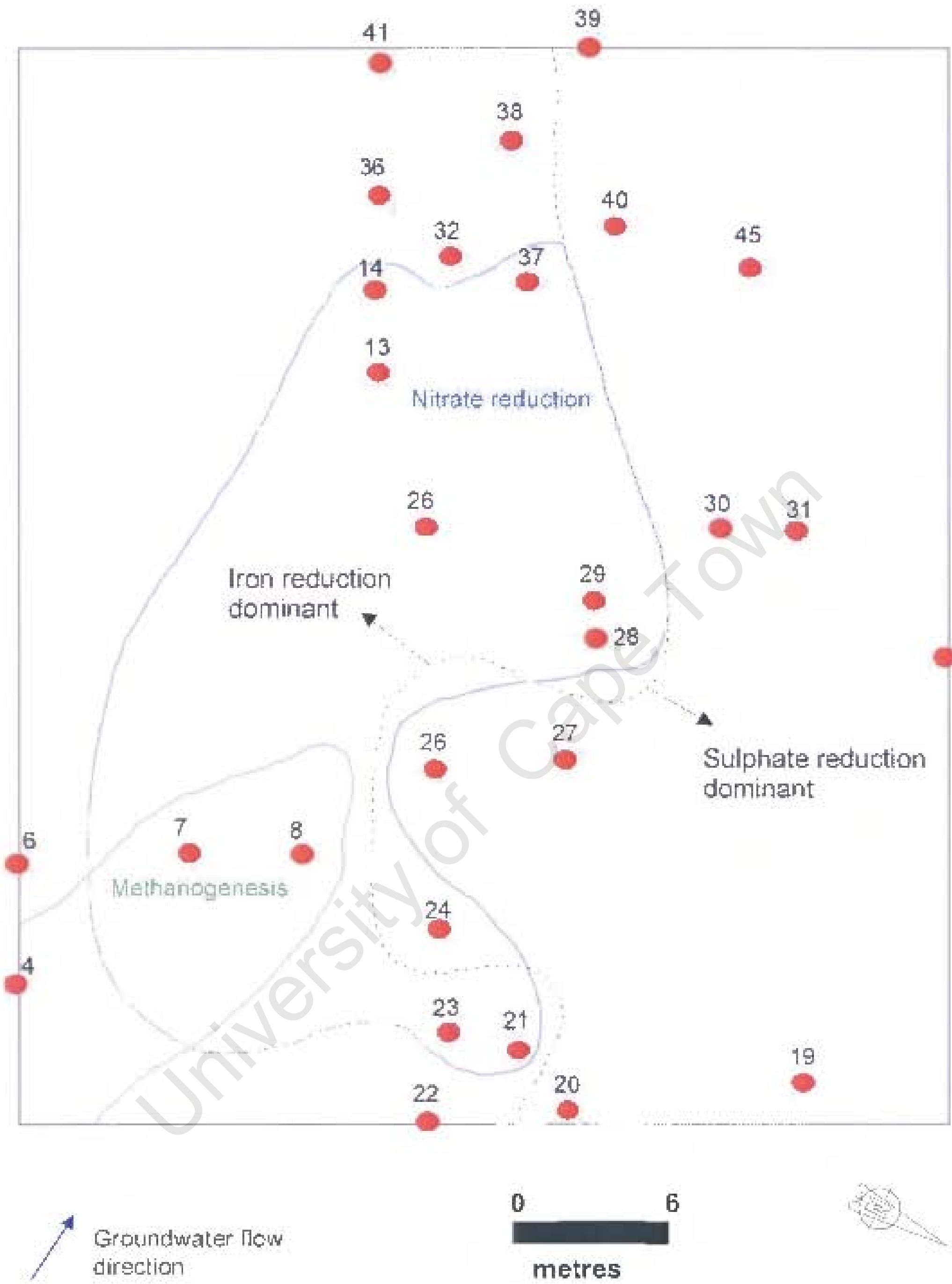

Figure 4.1. Schematic diagram showing the areas in which NO_3^- (blue line) and methanogenesis (green line) are thought to be occurring. The black stippled line indicates the areas in which it is thought that Fe^{3+} and SO_4^{2-} reduction are the dominant processes. It is important to note that this line does not represent separate areas where only Fe^{3+} or SO_4^{2-} reduction is occurring as these processes occur concomitantly.

University of Cape Town

2. KINETICS OF IRON AND SULPHATE REDUCTION

Samples GM26 and GM27 were chosen for the sediment incubations as GM26 had a Fe^{2+} concentration that was intermediate between the samples with the highest and lowest Fe^{2+} concentrations, while GM27 had a low Fe^{2+} concentration.

The variability in the pore water Fe^{2+} concentrations of GM26 and GM27 (Figures 3.4 and 3.5 respectively) can possibly be explained by comparing these plots with those of the pore water SO_4^{2-} concentrations in these sites (Figures 3.6 and Figure 3.7). Pore water Fe^{2+} concentrations did not increase consistently over the first 24 hours of the incubation in both GM26 and GM27. This may possibly be due to the precipitation of iron sulphides in the incubation sediments. In GM26, the lowest pore water Fe^{2+} concentration was measured after 6 hours and was accompanied by a rapid decrease in the pore water SO_4^{2-} concentrations. As Fe^{3+} and SO_4^{2-} are reduced, the Fe^{2+} is most probably removed from solution by precipitating out as iron sulphide. After 12 hours there is an increase in the concentration of Fe^{2+} and SO_4^{2-}. The increased Fe^{2+} concentrations can be explained if Fe^{3+} reduction continued over this period (from 6 to 12 hours), and SO_4^{2-} reduction was inhibited accounting for the increase in SO_4^{2-}. Precipitation of Fe^{2+} would thus be hindered and the concentration in the pore water would increase as is observed. Between 12 and 24 hours, the Fe^{2+} and SO_4^{2-} concentrations decrease again which is also most likely due to precipitation of iron sulphides.

2.1. Sulphate reduction

The highest measured concentration of SO_4^{2-} (1242 µM) in the groundwater was found at GM27, and is 3.7 times higher than the concentration at GM26 (333 µM). GM27 has a SRR of 178 nM.cm^{-3}.h^{-1}, while the SRR in GM26 is 83 nM.cm^{-3}.h^{-1} which is more than 2 times slower than the SRR in GM27. In a study carried out by Jakobsen and Postma (1999) on a shallow sandy aquifer, they found that organic matter reactivity has a much larger influence on the rate of sulphate reduction than the sulphate concentration. This was deduced from one of the sites where sulphate concentrations are low, but the measured SRR's are the highest. However, this is not the case at the current study site. As already mentioned, the fastest SRR is found at GM27 where the highest groundwater SO_4^{2-} concentration (1242 µM) was also measured. This implies that the SO_4^{2-} concentration rather than the reactivity of organic matter controls the rate of sulphate reduction. The sediments at the site contain very little natural organic matter. The organic matter found at the site is of the same type (i.e. petroleum hydrocarbons) and thus organic matter reactivity must also be the same across the site. Thus the reactivity of organic material is immaterial with respect to the SRR suggesting that SO_4^{2-} concentrations control the SRR.

Boudreau and Westrich (1984) investigated the effect of sulphate concentration on the rate of bacterial sulphate reduction in marine sediments from Long Island Sound. The results show that the rate is independent of the dissolved sulphate concentration until concentrations of < 3 mM are reached. SO_4^{2-} concentrations at the site are all less than 3 mM providing further evidence that the SO_4^{2-} concentration is controlling the SRR. The concentration of SO_4^{2-} at GM26 is lower than that found at GM27. This difference in the SO_4^{2-} concentrations at the two sites is used to account for the slower SRR found at GM26.

2.2. Iron reduction

The rates of iron reduction were determined by measuring the accumulation of extractable Fe^{2+} in the incubation sediments using 0.5 M HCl. This method has also been used by

University of Cape Town

Kostka *et.al.* (2002) to measure the FeRR in saltmarsh sediments at a site in Georgia. In GM26 the extractable Fe^{2+} does not increase over the 48-hour incubation period showing that precipitation of iron sulphides was not occurring.

In GM27 the extractable Fe^{2+} in the sediments increases. Linear regression of the data gives a FeRR of 99 $nM.cm^{-3}.h^{-1}$ which is almost half the SRR of 178 $nM.cm^{-3}.h^{-1}$ in GM27. The increase in the extractable Fe (II) over the incubation period means that precipitation of iron sulphides is occurring, and thus concomitant iron and sulphate reduction is occurring. This possibly explains why the Fe^{2+} measured in the groundwater at this site is low (Figure 3.1c), while there is an accumulation of sulphide in the water.

3. SEDIMENT EXTRACTIONS

3.1. Set 1 – Comparison of samples taken 40 cm below ground surface with samples taken from the depth of the water table

The main aim of this was to determine if there was a difference between the amount of iron oxides found in the sediments at a depth of 40 cm and the sediments taken at the depth of the water table. If higher concentrations of iron oxides occur in the vadose zone, and lower concentrations below the water table, this would be a clear indication that reduction of iron oxides found in the sediments was occurring. However this could only be used as an indication as to what might be happening at the site as geological heterogeneities will undoubtedly exist between sediments taken near the surface and those at depth.

University of Cape Town

The extractions performed showed that the extractable iron using the ascorbate solution was very similar in samples taken from the top and bottom in sample A. The extractable iron was slightly higher in the samples taken from the top showing that reserve of iron oxides in the sediment below the site has been lost. This loss is most likely due to the reduction of amorphous iron oxyhydroxides. In samples B, E, and 26, the extractable iron using the ascorbate was higher in the samples taken from the depth of the water table. The most plausible explanation for this occurrence is that the samples taken from a depth of 40 cm don't contain large amounts of iron oxyhydroxides, and that iron associated with the AVS in these samples was extracted from the samples taken near the water table. If this is the case then the precipitation of AVS is taking place which implies concomitant reduction of iron and sulphate.

The extractable iron using the sodium dithionite solution was very similar in samples taken from the top and near the water table for samples B, E, and 26. In all samples, the extractable iron using sodium dithionite was higher than when the ascorbate solution was used. The difference suggests that amorphous iron oxyhydroxides as well as crystalline iron oxide phases are extracted using sodium dithionite. Although these crystalline iron oxide phases are extracted using sodium dithionite, this does not necessarily mean that microbes found at the site have the potential to reduce these more stable iron oxides. Thus, although extracted, reduction of these phases may not be taking place and thus do not contribute to the degradation of the organics.

University of Cape Town

3.2. Set 2 – Measurement of total extractable iron and extractable Fe^{2+} from samples taken at the depth of the water table

Figure 3.3 shows that in all the samples taken from a depth just below the water table, the total extractable iron and the extractable Fe^{2+} are very similar in all samples. From this it can be said that most of the extractable iron is in the reduced form and not the oxidised form. These reduced phases are either likely to be FeS (mackinawite and amorphous FeS) or FeS_2 (pyrite).

4. ALKALINITY

The alkalinity of background groundwater samples is very high (between 8.5 and 9.5). These high background alkalinities so far have not been explained. Dissolution of calcite by groundwater moving through the Langebaan (Aeolian, calcrete capped calcareous sandstone) and Witzand (Aeolian, calcareous, quartzose sand) Formations is possibly taking place resulting in higher alkalinities. However, it is still thought to be unlikely that calcite dissolution that may be taking place in the aquifer could account for these unusually high alkalinities. Ca^{2+} concentrations in background samples are notably higher than in samples taken from within the plume indicating the processes within the plume are removing Ca^{2+} from the groundwater. However this is the opposite to what should be observed because as the pressure of CO_2 increases as a result of microbial respiration, the alkalinity and the concentration of Ca^{2+} increase due to the dissolution of calcite if present (Stumm & Morgan, 1996). Ion exchange processes may be occurring removing Ca^{2+} from solution.

University of Cape Town

4.1. Species contributing to alkalinity

The CO_2 produced by respiring microbes during denitrification as well as sulphate and iron reduction, will dissolve to form carbonic acid through the reaction:

$$CO_2 + H_2O \rightarrow H_2CO_3$$

The measured groundwater pH at the site ranges between 6.5 and 7.1 in the contaminated groundwater, except at GM4 where the measured pH is 6.1. For pH values in this range, the carbonic acid produced will dissociate to form H^+ and HCO_3^- through the reaction:

$$H_2CO_3 \rightarrow H^+ + HCO_3^-$$

The overall CO_2 dissolution reaction can be written as:

$$CO_2 + H_2O \rightarrow H^+ + HCO_3^-$$

At these measured pH's, hydrogen sulphide produced during sulphate reduction will also dissociate as follows:

$$H_2S \rightarrow H^+ + HS^-$$

Thus it can be said that the main species contributing to the alkalinity at the site are HCO_3^- and HS^-.

The processes of NO_3^-, Mn^{4+}, Fe^{3+}, and SO_4^{2-} reduction all generate alkalinity and the alkalinity generated by these process based on a moles per mole stoichiometric turnover is shown in Table 4.1. Biodegradation of hydrocarbons under aerobic and methanogenic

University of Cape Town

conditions do not produce alkalinity. It would therefore be expected that the alkalinity should increase in the contaminant plume under the conditions that have been identified to be taking place at the site (NO_3^-, Fe^{3+} and SO_4^{2-} reduction). This however has not been observed at the site. The alkalinities were only higher at GM4, GM7, and GM8 compared to background samples. The remainder of the samples taken either had alkalinities that were similar or lower than background samples and the reasons for this are unknown.

4.2. Comparison of alkalinities determined using colourimetry and titration

The results obtained from the colourimetric determination of total alkalinity yielded unexpectedly high values. As a result thereof, it was thought that the colourimetric method of Sarazin (1999) used may contain a bias. The alkalinities of five samples (GM32, GM35, GM37, GM38, and GM39) were determined using by titration using 0.05 M HCl. The titration was performed using a pipette and the sample was stirred continuously using a magnetic stirrer. The titration data was entered into the United States Geological Survey web based alkalinity calculator. The concentrations of HCO_3^- calculated using this method are shown in Table 4.2.

Samples GM32, GM37, GM38, and GM39 generally show that the two methods give results that are within 14 %. Alkalinities using the spectrophotometric method were shown to give results that are within 1 % of the conventional Gran method (Sarazin, 1999). However, the results shown in Table 4.2 show large differences. In all of the above mentioned cases, the alkalinity determined spectrophotometrically is higher than the alkalinity determined using the Gran titration. This can be explained by the fact that chemical reaction that develops using the method of Sarazin (1999) develops immediately thereby minimising the oxygen contamination and redox interference reactions that alter the original sample alkalinity.

University of Cape Town

Table 4.1. Contributions to alkalinity of redox processes involved in hydrocarbon mineralization (Hunkeler *et al.*, 1999).

Process	**Contribution to alkalinity** [a]
Microbial hydrocarbon mineralisation [b]	
$0.68\ CH_{1.85} + \mathbf{O_2} \rightarrow 0.68\ CO_2 + 0.63\ H_2O$	0
$0.85\ CH_{1.85} + \mathbf{NO_3^-} + H^+ \rightarrow 0.85\ CO_2 + 0.5\ N_2 + 1.29\ H_2O$	+1
$0.34\ CH_{1.85} + MnO_{2(s)} + 2\ H^+ \rightarrow 0.34\ CO_2 + \mathbf{Mn^{2+}} + 1.31\ H_2O$	+2
$0.17\ CH_{1.85} + FeOOH_{(s)} + 2\ H^+ \rightarrow 0.17\ CO_2 + \mathbf{Fe^{2+}} + 1.66\ H_2O$	+2
$1.37\ CH_{1.85} + \mathbf{SO_4^{2-}} + 2\ H^+ \rightarrow 1.37\ CO_2 + H_2S + 1.26\ H_2O$	+2
$1.37\ CH_{1.85} + 0.74\ H_2O \rightarrow 0.37\ CO_2 + \mathbf{CH_4}$	0
Geochemical processes	
$CaCO_{3\ (s)} + 2\ H^+ \leftrightarrow CO_2 + \mathbf{Ca^{2+}} + H_2O$	+2
$2/3\ FeOOH_{(s)} + H_2S \rightarrow 2/3\ FeS_{(s)} + 1/3\ S^0 + 4/3\ H_2O$	0
$CO_2 + Fe^{2+} + H_2O \leftrightarrow FeCO_{3\ (s)} + 2\ H^+$	-2

[a] Moles per mole stoichiometric turnover
[b] Average H / C ratio in diesel fuels of 1.85. All species given in the form in which they exist a the reference point of the alkalinity titration (pH=4.3). Tthus, the number of proton produced or consumed corresponds to alkalinity consumption or production. The species printed in bold were used to quantify the processes.

Table 4.2. Comparison of alkalinities for samples GM23, GM35, GM37, GM38, and GM39 determined using the methods of Sarazin (1999) and by titration using 0.05 M HCl. All units of alkalinities are expressed as mM.

	GM32	**GM35**	**GM37**	**GM38**	**GM39**
Total alkalinity [a]	9.0	1.9	6.3	8.9	8.5
Bicarbonate [b]	7.5	3.6	5.4	7.8	7.2
Difference [c]	1.5 (17)	1.7 (47)	0.9 (14)	1.1 (12)	1.3 (15)

[a] Determined using the method of Sarazin (1999)
[b] Bicarbonate concentration from USGS web based alkalinity calculator using the Theoretical Carbonate Titration Curve Method 2
[c] Values in brackets show difference expressed as %

University of Cape Town

The Gran titrations were performed in the lab on returning from the field at the end of the day. The alkalinity of these samples may therefore be expected to be lower for the following reasons. Despite keeping the samples under anaerobic conditions in the field and during transport, the titrations were performed in the open. This may have resulted in the oxidation of some of the species (e.g. sulphides) that contribute to alkalinity. Another reason for this is that the amount of CO_2 outgassing from these samples would have been greater than that which would have occurred in the samples to which the reagents were added in the field.

GM35 shows a 47 % difference in the alkalinities determined by the two different methods. The alkalinity of this sample using the spectrophotometric method is grossly underestimated. The electroneutrality calculated using the alkalinity determined spectrophotometrically (Appendix C) results in an excess of cations by 23 %. Using the bicarbonate alkalinity from the Gran titration data, the electroneutrality was calculated as -6 % showing that the alkalinity determined from the titration data this is a far more accurate reflection of the true alkalinity.

University of Cape Town

5. PH

An unexpected observation was that the pH tended to be lower in the pollution plume than in the background samples. Most of the reactions oxidising the organic material within the plume consume H^+ and produce alkalinity and thus the pH should be higher in the pollution plume. A possible reason for the reversal of the trend is that precipitation of HCO_3^- occurs along with iron removing alkalinity from the water. The decrease in the pH found at this site cannot be explained.

6. IMPLICATIONS FOR FUTURE SITE REMEDIATION

The results obtained from this study have significant implications regarding the possibilities for remediation activities at the site, and the ways in which this may be enhanced. *In situ* treatment can either involve physical, chemical, or biological treatment. As the focus of this project has been to determine the processes contributing to biodegradation at the site, *in situ* biological treatment will be briefly discussed. Boulding (1995) describes two basic approaches to *in situ* biodegradation. The first relies on the natural biological activity in the subsurface, such as that which is taking place at this site, and involves minimal intervention. All of the available TEA's (NO_3^-, Fe^{3+}, and SO_4^{2-}) are the limiting factors for hydrocarbon degradation. It is therefore necessary to use the second approach described by Boulding (1995) called enhanced biorestration. This involves stimulating the existing microorganisms by the addition of nutrients (nitrogen and phosphorous) and TEA's.

Two *in situ* biological treatments are considered to be appropriate in order to stimulate microbial hydrocarbon biodegradation. Air sparging involves putting injection and recovery wells in place to induce circulation of nutrients through the contaminated portion of the aquifer. Oxygen can then be supplied by sparging air into the injection wells (Boulder, 1995). Air sparging in the saturated zone serves a two-fold purpose (Anderson, 1995): it provides oxygen, which acts as an electron acceptor for biodegradation in the aquifer and the unsaturated zone, and it physically transfers volatile substances to the unsaturated zone. These volatiles can then be captured by an *in situ* vapour recovery system. Dissolved oxygen is distributed through the aquifer by movement of air bubbles, diffusion, and groundwater movement. Liquid delivery systems are used to add TEA's and inorganic nutrients to enhance biodegradation of the contaminants (Anderson, 1995). The delivery system (wells or trenches) functions to circulate adequate amounts of nutrients and oxygen

University of Cape Town

through the zone of contamination. Injection wells are placed within or close to the contaminated area. Groundwater extraction wells or trenches may be included. The produced groundwater is extracted, treated above ground if necessary, and then disposed or amended with nutrients and re-circulated. This is particularly of significance as nitrate, sulphate, and salts of Fe^{3+} can act as alternate electron acceptors. Hydrogen peroxide is an alternative source of oxygen that may be used (Boulder, 1995). Iron or an organic catalyst is used to decompose hydrogen peroxide to oxygen. However, the rate at which hydrogen peroxide decomposes to oxygen must be controlled to limit the formation of bubbles. These bubbles can lead to a gas blockage and thus reduce permeability. Another problem with the use of hydrogen peroxide is that it may mobilise metals such as lead and antimony. In hard waters, magnesium and calcium phosphates can precipitate and plug injection wells. The addition of sulphate as an electron acceptor has several advantages over aerobic bioremediation (Anderson & Lovley, 2000). It does not react with reduced metabolites such as Fe^{2+} or S^{2-}, and unlike oxygen, is not consumed by abiological processes unrelated to hydrocarbon degradation. Sulphate is also more soluble than oxygen and has twice the electron accepting capacity of oxygen. Furthermore, sulphate does not result in the plugging of the aquifer with precipitated iron oxides.

Temperature, pH, and nutrient supply can influence biodegradation. The optimum temperature for the growth of microorganisms present in shallow aquifers is between 25°C and 40°C. Anaerobic microorganisms are sensitive to pH and operate efficiently in a narrow pH range with biodegradation rates being optimum between pH 7 and 8 (Norris *et al.*, 1994). Biodegradation may be inhibited if the pH falls outside of a specified range (pH 5 to 9). During field measurements, groundwater temperatures were usually between 18°C and 20°C which is slightly lower than the optimum temperature for microbial growth. These

University of Cape Town

temperatures would increase slightly during the summer months providing an ideal temperature for microbial growth. The pH of the groundwater is neutral to slightly acidic and pH conditions are thus also almost ideal for optimum anaerobic biodegradation rates.

7. GROUNDWATER SATURATION INDICES USING PHREEQC

Mineral saturation indices (SI = log(IAP / K(T))) at various sites were calculated in PHREEQC using the WATEQ4F database (Table 4.3). Due to the fact that iron in the groundwater is almost predominantly present as Fe^{2+} at the measured pH, the iron concentration was entered into the PHREEQC input file as Fe^{2+} and not total Fe.

Table 4.3. Saturation index values for groundwater at various sites calculated using PHREEQC and the WATEQ4F database. Background samples are shown in red text.

Well No.	Calcite ($CaCO_3$)	Siderite ($FeCO_3$)	Mackinawite (FeS)	Amorphous FeS	Pyrite (FeS_2)
GM4	-0.67	1.18	0.68	-0.05	21.96
GM8	0.11	1.59	1.82	1.09	24.58
GM13	-0.20	1.36	1.32	0.59	23.59
GM19	-0.71	0.13	1.42	0.69	24.66
GM21	0.26	1.74	2.16	1.43	25.29
GM27	0.13	0.24	1.37	0.64	25.19
GM31	-0.08	0.93	1.69	0.96	24.94
GM36	-0.53	0.92	1.72	0.99	24.62
GM39	-0.01	0.56	1.21	0.48	24.28
GM45	0.02	0.43	1.57	0.83	25.15
GM48	0.53	-0.65	-0.68	-1.41	22.17
GM49	0.30	-0.84	-1.07	-1.81	21.37
GM50	0.42	-0.79	-0.88	-1.61	21.76

Background samples GM48, GM49, and GM50 are all undersaturated with respect to both the amorphous and crystalline iron sulphide minerals as well as siderite ($FeCO_3$). However,

University of Cape Town

the background groundwater is oversaturated with respect to calcite and this may help to account for the high background alkalinities. This may arise from the dissolution of calcite and shell fragments in other formations through which the groundwater has moved and been in contact with as suggested above. The lower saturation indices with respect to calcite in samples located within the plume is most probably related to the lower concentrations of Ca^{2+} found in samples within the plume compared to background samples.

Samples taken from within the plume are oversaturated with respect to mackinawite, amorphous FeS, and pyrite. This confirms previous thinking that concomitant Fe^{3+} and SO_4^{2-} reduction are occurring. Cozzarelli *et.al.* (1999) suggest that the presence of organic acids in groundwater may complicate the solubility controls of iron. The Fe^{2+} in the groundwater may not all be present as uncomplexed ions and that a component of the Fe^{2+} complexed to organic-acid anions may be present. Thus, it is thought that the oversaturation calculated for the groundwater with respect to iron-sulphide minerals may only be an apparent oversaturation.

Removal of alkalinity from the groundwater may be occurring via the formation of siderite ($FeCO_3$). The oversaturation of the groundwater with respect to siderite suggests that this is possible and siderite may be precipitating in the sediments. However, a more detailed sediment analysis of the sediments is required to confirm this. In a studies carried out by Cozzarelli *et al.* (1999) and Tuccillo *et al.* (1999), siderite and ferroan calcite reported in the anoxic zones of a shallow aquifer containing high concentrations of dissolved hydrocarbons, Fe^{2+}, and HCO_3^-. This is a similar situation to that which exists at this site and could therefore be an important process removing iron and alkalinity in the form of HCO_3^-.

University of Cape Town

CHAPTER 5 - CONCLUSIONS AND RECOMMENDATIONS

1. CONCLUSIONS

Aerobic biodegradation has ceased resulting in anaerobic groundwater conditions at the site. This can be concluded based on the elevated concentrations of reduced species such as NH_4^+, Fe^{2+}, and ΣH_2S, and the removal of NO_3^- and SO_4^{2-} from the groundwater. These factors undoubtedly reflect that anaerobic biodegradation of the hydrocarbons is taking place. The main processes contributing to hydrocarbon degradation are NO_3^-, Fe^{3+}, and SO_4^{2-} reduction. Mn^{4+} reduction, based on the low concentrations of extractable Mn from sediments taken above the water table, is not considered to play a significant role in hydrocarbon degradation at the site.

The most reduced conditions are found closest to where the product spillage occurred. The highest concentrations of Fe^{2+} are also found here and thus Fe^{3+} reduction is the dominant process occurring close to spillage position. Further away SO_4^{2-} reduction becomes the dominant process and has resulted in the accumulation of ΣH_2S in the groundwater. The redox zonation based on thermodynamic principles that has been observed in other studies is difficult to distinguish at this site. This is due to the fact that there is evidence for concomitant NO_3^-, Fe^{3+} and SO_4^{2-} reduction at the site. Concomitant Fe^{3+} and SO_4^{2-} reduction has resulted in the removal of Fe^{2+} and ΣH_2S from solution through the precipitation of iron sulphides. Modelling in PHREEQC shows that groundwater in the contaminant plume is saturated with respect to mackinawite, amorphous FeS, pyrite, and siderite. Further investigations are required to confirm the presence of phases such as siderite.

University of Cape Town

Due to the sandy nature of the aquifer it is expected to contain very little natural organic matter and the reactivity of organic mater is therefore not considered to be significant in determining the SRR and FeRR as all the organic matter found at the site is of the same type i.e. petroleum hydrocarbons. Based on sediment incubation experiments carried out on two samples, the highest SRR is found to occur at the site where the groundwater SO_4^{2-} concentrations are the highest. Furthermore, groundwater SO_4^{2-} concentrations are lower than 3 mM. Boudreau and Westrich (1984) found that the SRR was independent of the dissolved SO_4^{2-} until levels of < 3 mM are reached. The SO_4^{2-} concentration in the groundwater therefore determines the SRR.

The availability of TEA's, and not organic matter is concluded to be the limiting factor for hydrocarbon biodegradation. Thus, if any *in situ* biological remedial activities are to be conducted at the site to enhance the rate of biodegradation then the addition of TEA's such as NO_3^- and SO_4^{2-} will be required.

There are however a couple of issues that remain unresolved at this stage. The first of these is the very high alkalinities found at the site. The second is the fact that pH and alkalinities within the plume have not increased as has been found by numerous other studies of a similar nature.

2. Recommendations for further studies

- Additional groundwater sampling events should take place during summer months in order to gain some insight into how redox processes are affected on a seasonal basis.

University of Cape Town

- A detailed study of the sediments at the site is recommended to identify the reduced iron phases precipitating in the sediments. The presence of siderite or ferroan calcite may help to explain some of the processes occurring. A study of iron sulphides will provide insight into whether pyrite formation occurs via a FeS precursor or by direct precipitation processes. An analysis of the sediments using a scanning electron microscope would reveal if iron oxide surfaces are coated with reduced iron phases thereby limiting iron reduction and allowing sulphate reduction to become favourable.

- Additional experiments can be run to determine if amendments using SO_4^{2-} and NO_3^- enhance the rates of hydrocarbon degradation. It is advisable to perform these experiments at a laboratory scale first. This would help in the decision making process as to which remedial option should be followed. Thereafter, depending on the success of the laboratory experiments, amendments to the aquifer itself can be investigated.

University of Cape Town

REFERENCES

Aelion, C.M. (1996). Impact of aquifer sediment grain size on petroleum hydrocarbon distribution and biodegradation. *Journal of Contaminant Hydrology,* **22,** 109-121.

Anderson, R.T. and Lovley, D.R. (2000). Anaerobic bioremediation of benzene under sulfate-reducing conditions in a petroleum-contaminated aquifer. *Environmental Science and Technology,* **34,** 2261-2266.

Anderson, W.C. (1995). Innovative site remediation technology. Springer-Verlag, Berlin. 288pp.

Appelo, C.A.J., and Postma, D. (1994). *Geochemistry, groundwater and pollution.* A.A. Balkema, Rotterdam. 536 pp.

Baedecker, M.J. and Back, W. (1979). Modern marine sediments as a natural analog to the chemically stressed environment of a landfill. *Journal of Hydrology,* **43,** 393-414.

Birch, G.F. (1981). The Karbonat-Bombe: A precise, rapid and cheap instrument for determining calcium carbonate in sediments and rocks. *Transactions of the Geological Society of South Africa,* **84,** 199-203.

Bjerg, P.L., Rűgge, K., Pedersen, J.K., and Christensen, T.H. (1995). Distribution of redox sensitive groundwater quality parameters downgradient of a landfill (Grindsted, Denmark). *Environmental Science and Technology,* **29,** 1387-1394.

Borden, R.C. (1994). Natural bioremediation of hydrocarbon-contaminated ground water. In: *Handbook of Bioremediation.* Ed., Norris, Hinchee, Brown, McCarty, Semprini, Wilson, Kampbell, Reinhard, Bouwer, Boren, Vogel, Thomas, and Ward. CRC Press, Inc. Florida.

Borden, R.C., Gomez, C.A, and Becker, M.T. (1995). Geochemical indicators of intrinsic bioremediation. *Ground Water,* **33,** 180-189.

Boudreau, B.P. and Westrich, J.T. (1984). The dependence of bacterial sulfate reduction n sulfate concentration in marine sediments. *Geochemica et Cosmochimica Acta,* **48,** 2503-2516.

University of Cape Town

Boulding, J.R. (1995). Practical handbook of soil, vadose zone, and ground-water contamination: assessment, prevention and remediation. CRC Press, Inc., Florida. 948 pp.

Bulger, P.R., Kehew, A.E., and Nelson, R.A. (1989). Dissimilatory nitrate reduction in a waste-water contaminated aquifer. *Ground Water,* **27,** 664-671.

Champ, D.R., Gulens, J., and Jackson, R.E. (1979). Oxidation-reduction sequences in ground water flow systems. *Canadian Journal of Earth Science,* **16,** 12-23.

Chapelle, F., and Lovley, D.R. (1992). Competitive exclusion of sulfate reduction by Fe(III)-reducing bacteria: a mechanism for producing discrete zones of high-iron ground water. *Ground Water,* **30,** 29-36.

Chapelle, F.H. (1993). *Ground-water microbiology and geochemistry.* John Wiley and Sons, Inc. New York.

Chapelle, F.H., Haack, S.K., Adriaens, P., Henry, M.A., and Bradley, P.M. (1996). Comparison of Eh and H_2 measurements for delineating redox processes in a contaminated aquifer. *Environmental Science and Technology,* **30,** 3565-3569.

Christensen, T.H., Bjerg, P.L., Banwart, A., Jakobsen, R., Heron, G., Albrechtsen, H. (2000). Characterization of redox conditions in groundwater contaminated plumes. *Journal of Hydrology,* **45,** 165-241.

Cline, J.D. (1969). Spectrophotometric determination of hydrogen sulfide in natural waters. *Limnology and Oceanography,* **14,** 454-458.

Coleman, M.L., Hedrick, D.B., Lovley, D.R., White, D.C, and Pye, K. (1993). Reduction of Fe(III) in sediments by sulphate-reducing bacteria. *Nature,* **361,** 436-438.

Cozzarelli, I.M., Herman, J.S., Baedecker, M.J., Fischer, J.M. (1999). Geochemical heterogeneity of a gasoline-contaminated aquifer. *Journal of Contaminant Hydrology,* **40,** 261-284.

Cozzarelli, I.M., Bekins, B.A., Baedecker, M.J., Aiken, G.R., Eganhouse, R.P., and Tuccillo, M.E. (2001). Progression of natural attenuation processes at a crude-oil spill site: I. Geochemical evolution of the plume. *Journal of Contaminant Hydrology,* **53,** 369-385.

Fetter, C.W. (1999). *Contaminant hydrogeology, 2nd edition.* Prentice-Hall Inc. New Jersey.

University of Cape Town

Heron, G., Bjerg, P.L., Gravesen, P., Ludvigsen, L., Christensen, T.H. (1998). Geology and sediment geochemistry of a landfill leachate contaminated aquifer (Grindsted, Denmark). *Journal of Contaminant Hydrology,* **29,** 301-317.

Hunkeler, D., Höhener, P., Bernasconi, S., and Zeyer, J. (1999). Engineered *in situ* bioremediation of a petroleum hydrocarbon-contaminated aquifer: assessment of mineralization based on alkalinity, inorganic carbon and stable carbon isotope balances. *Journal of Contaminant Hydrology,* **37,** 201-223.

Jakobsen, R., and Postma, D. (1999). Redox zoning, rates of sulfate reduction and interactions with Fe-reduction and methanogenesis in a shallow sandy aquifer, Rømø, Denmark. *Geochemica et Cosmochimica Acta,* **63,** 137-151.

Kostka, J.E., Roychoudhury, A., and Van Cappellen, P. (2002). Rates and controls of anaerobic microbial respiration across spatial and temporal gradients in saltmarsh sediments. *Biogeochemistry,* **60,** 49-76.

Krumholz, L.R., Caldwell, M.E., and Suflita J.M. (1996). Biodegradation of 'BTEX' hydrocarbons under anaerobic conditions. *In: Bioremediation: Principles and applications.* Ed. Crawford R.L., and Crawford, D.L. Cambridge University Press, Great Britain.

Lindberg, R.D., and Runnells, D.D. (1984). Ground water redox reactions: an analysis of equilibrium state applied to Eh measurements and geochemical modelling. *Science,* **225,** 925-927.

Lovley, D.R., and Goodwin, S. (1988). Hydrogen concentrations as an indicator of the predominant terminal electron-accepting reactions in aquatic sediments. *Geochimica et Cosmochimica Acta,* **52,** 2993-3003.

Ludvigsen, L., Albrechtsen, G., Heron, G., Bjerg, P.L., Christensen, T.H. (1998). Anaerobic microbial redox processes in a landfill leachate contaminated aquifer (Grindsted, Denmark). *Journal of Contaminant Hydrology,* **33,** 273-291.

Lyngkilde, J., and Christensen, T.H. (1992). Redox zones of a landfill leachate pollution plume (Vejen, Denmark). *Journal of Contaminant Hydrology,* **10,** 273-289.

McBride, B. (2001). Kantey & Templer Project No. 81201GC. Engen: ex Toyota Supra contamination assessment interim progress report. Period 1 February – 21 December 2001.

University of Cape Town

Meyer, P.S. (2000). *An explanation of the 1:500 000 general hydrogeological map Cape Town 3317.* Department of Water Affairs and Forestry. 59 pp.

Norkus, R.G., Maurer, J., Schults, N.A., and Stuart, J.D. (1996). Field examination of ground water quality as an indicator of microbiological activity at gasoline contaminated sites. *Chemosphere,* **33,** 421-436.

Postma, D., and Jakobsen, R. (1996). Redox zonation: Equilibrium constraints on the Fe(III)/SO_4-reduction interface. *Geochemica et Cosmochimica Acta,* **60,** 3169-3175.

Reid, D.L., Rogers, J. and Hartnady, C.J. (1998). *International Volcanological Congress field excursion guidebook. Geology of the Cape Peninsula.* Department of Geological Sciences, University of Cape Town, Rondebosh, South Africa. 51 pp.

Sarazin, G., Michard, G., and Prevot, F. (1999). A rapid and accurate spectroscopic method for alkalinity measurements in sea water samples. *Water research,* **33,** 290-294.

Solorzano, L. (1969). Determination of ammonia in natural water by the phenol-hypochlorite method. *Limnology and Oceanography,* **14,** 799-801.

South African Weather Bureau (1996). The weather and climate of the south-western Cape. Department of Environmental Affairs and Tourism, Pretoria.

Stookey, L.L. (1970). Ferrozine – a new spectrophotometric reagent for iron. *Analytical Chemistry,* **42,** 779-781.

Stumm, W., and Morgan, J.J. (1996). *Aquatic chemistry. 3rd edition.* John Wiley and Sons, New York. 1022 pp.

Tabababi, M.A. (1974). A rapid method for the determination of sulphate in water samples. *Environmental Letters,* **7,** 237-243.

Theron, J.N. (1984). The geology of Cape Town and Environs. Explanation sheets 3318 CD and DC, and 3418 AB, AD, and BA. Geological Survey of South Africa. 77 pp.

Theron, J.N., Gresse, P.G., Siegfried, H.P., and Rogers, J. (1992). *The geology of the Cape Town area. Explanation of the 1:250 000 sheet 3318.* Geological Survey of South Africa. 140 pp.

University of Cape Town

Tuccillo, M.E., Cozzarelli, I.M., Herman, J.S. (1999). Iron reduction in the sediments of a hydrocarbon contaminated aquifer. *Applied Geochemistry,* **14,** 655-667.

Van der Merwe, W. (2000). Kantey & Templer Project No. 81201GC. Contamination assessment report.

University of Cape Town

APPENDIX A - AERIAL PHOTOGRAPH OF SITE

University of Cape Town

0 20
metres

APPENDIX B - TABULATED RESULTS OF ANALYTICAL DATA

University of Cape Town

Table B1. Results from measurements performed in the field as well as the measured alkalinity of all samples.

Well No	pH	EC (µS/cm)	Eh (mV)	Alkalinity (mM)
GM 4	6.1	1220	-96	10.1
GM 6	6.7	965	-96	9.2
GM 7	6.6	1058	-102	10.0
GM 8	6.8	1286	-106	10.1
GM 13	6.6	1035	-96	9.2
GM 14	6.7	977	-105	8.0
GM 19	6.6	775	-108	4.1
GM 20	6.7	1094	-92	6.8
GM 21	7.0	1336	-161	9.9
GM 22	6.6	1090	-72	8.1
GM 23	6.6	784	-91	6.4
GM 24	6.7	932	-125	8.4
GM 25	6.7	1087	-83	6.8
GM 26	6.8	1077	-118	8.9
GM 27	7.1	1549	-129	7.5
GM 28	6.8	1058	-96	9.1
GM 29	6.8	1010	-109	8.9
GM 30	6.5	391	-126	3.9
GM 31	6.9	1436	-221	6.9
GM 32	6.7	1095	-99	9.0
GM 35	6.8	307	120	1.9
GM 36	6.6	635	-88	5.9
GM 37	6.5	940	-13	6.3
GM 38	6.8	1075	-94	8.9
GM 39	6.8	915	-76	8.5
GM 40	6.9	1201	-78	9.6
GM 41	6.7	1059	-85	8.2
GM 44	6.7	1135	-23	5.6
GM 45	6.7	1028	-138	9.2
GM 48	7.2	1466	42	9.3
GM 49	7.0	1497	62	8.5
GM 50	7.0	1533	53	9.5

University of Cape Town

Table B2. Groundwater anion concentrations from the sampled well points. All concentrations are in μM.

Well No	SO_4^{2-} [a]	ΣH_2S [a]	NO_3^- [a]	Cl^- [a]	F^- [a]	Br^- [a]
GM 4	*	1.8	*	1159	169	92
GM 6	144	1.8	55	1073	142	52
GM 7	143	3.1	*	1047	152	80
GM 8	246	3.2	*	1180	218	121
GM 13	131	1.9	188	1643	143	25
GM 14	102	3.7	210	1472	148	29
GM 19	475	19.6	27	2411	111	17
GM 20	437	4.6	305	2982	*	43
GM 21	380	4.3	464	1811	172	10
GM 22	256	2.1	369	1976	152	1
GM 23	182	4.0	91	1991	131	16
GM 24	201	6.5	105	1326	209	28
GM 25	745	13.5	208	2475	151	11
GM 26	333	6.5	73	2075	185	57
GM 27	1242	12.4	120	4883	200	13
GM 28	197	4.2	75	1688	148	49
GM 29	165	4.3	331	1582	156	20
GM 30	39	25.3	20	357	76	24
GM 31	529	6.3	318	6067	191	1
GM 32	164	15.7	341	1990	146	23
GM 35	43	1.2	21	189	36	4
GM 36	51	9.8	*	1142	124	18
GM 37	273	2.5	1164	1755	139	12
GM 38	189	4.9	61	2333	140	47
GM 39	222	7.0	75	1751	160	52
GM 40	372	10.5	39	3251	*	41
GM 41	169	3.8	57	2487	138	30
GM 44	670	3.4	191	3702	146	1
GM 45	105	24.0	*	1749	173	79
GM 48	1119	1.0	1185	2651	200	5
GM 49	1360	0.7	1164	2929	*	24
GM 50	1072	0.8	645	2319	212	13

[a] - All concentrations expressed as μM

* - Not detected

University of Cape Town

Table B3. Major cation concentrations of all sampled well points.

Well No	Mn^{2+} [a]	NH_4^{+} [a]	Ca^{2+} [a]	Mg^{2+} [a]	K^{+} [a]	Na^{+} [a]	Fe^{2+} [a]
GM 4	6.4	202	3319	325	598	1636	978
GM 6	4.6	167	2595	592	352	1770	265
GM 7	2.2	401	2695	391	418	1970	496
GM 8	4.4	405	3593	535	564	2623	762
GM 13	8.4	287	2795	490	331	1940	678
GM 14	1.5	280	2745	461	428	1779	496
GM 19	0.4	77	1914	366	199	2932	38
GM 20	0.4	138	3069	597	293	3758	387
GM 21	2.7	421	3618	918	357	2336	724
GM 22	0.4	208	2894	597	307	2701	469
GM 23	0.7	155	1821	440	257	2397	556
GM 24	2.7	432	2795	580	379	2619	221
GM 25	1.3	162	2438	761	356	3732	139
GM 26	2.2	276	2695	498	387	3493	346
GM 27	0.7	105	2795	1428	288	6133	14
GM 28	3.8	355	2745	527	326	3406	498
GM 29	3.1	399	2944	461	340	1949	510
GM 30	1.5	109	1243	206	143	644	204
GM 31	2.4	170	2570	872	322	6307	55
GM 32	3.8	176	3019	584	377	3310	367
GM 35	0.4	3	689	107	105	1875	6
GM 36	1.5	156	1999	370	244	1962	348
GM 37	2.7	308	2745	292	390	2462	294
GM 38	3.5	146	2645	605	398	2910	503
GM 39	1.5	102	3443	588	348	2075	152
GM 40	2.7	174	3169	683	391	3610	25
GM 41	1.8	75	2458	634	379	2684	268
GM 44	1.8	132	*	769	263	3436	118
GM 45	1.5	177	3418	597	302	2223	31
GM 48	0.4	5	4716	671	849	3475	0
GM 49	2.2	3	4466	753	349	3667	0
GM 50	4.7	4	4965	815	373	3615	0

[a] - All concentrations expressed as μM
* - Results not received from lab

University of Cape Town

APPENDIX C - ANALYTICAL APPRAISAL: ELECTRONEUTRALITY

University of Cape Town

Table C1. Electroneutrality (EN) calculated using PHREEQC from analytical data in Appendix 1.

Sample No	EC (µS/cm)	EC/100(µS/cm)	EN (%)
GM 4	1220	12.2	4.43
GM 6	965	9.65	-5.71
GM 7	1058	10.58	-4.79
GM 8	1286	12.86	4.38
GM 13	1035	10.35	-8.16
GM 14	977	9.77	-5.40
GM 19	775	7.75	1.57
GM 20	1094	10.94	1.06
GM 21	1336	13.36	-0.46
GM 22	1090	10.9	-18.35
GM 23	784	7.84	-6.10
GM 24	932	9.32	-1.15
GM 25	1087	10.87	-4.27
GM 26	1077	10.77	-3.86
GM 27	1549	15.49	-2.08
GM 28	1058	10.58	-1.27
GM 29	1010	10.1	-9.90
GM 30	391	3.91	-4.21
GM 31	1436	14.36	-5.79
GM 32	1095	10.95	-6.47
GM 35	307	3.07	22.76
GM 36	635	6.35	2.74
GM 37	940	9.4	-18.52
GM 38	1075	10.75	-7.95
GM 39	915	9.15	-2.18
GM 40	1201	12.01	-9.52
GM 41	1059	10.59	-8.80
GM 44	1135	11.35	[a]
GM 45	1028	10.28	-2.47
GM 48	1466	14.66	-13.60
GM 49	1497	14.97	-15.10
GM 50	1533	15.33	4.74

[a] – Ca^{2+} results not received and thus the EN could not be calculated

University of Cape Town